HHS Public Access

Author manuscript

Sci Transl Med. Author manuscript; available in PMC 2024 December 06.

Published in final edited form as:

Sci Transl Med. 2023 December 06; 15(725): eadh7668. doi:10.1126/scitranslmed.adh7668.

USP2 inhibition prevents infection with ACE2-dependent coronaviruses in vitro and is protective against SARS-CoV-2 in mice

Fabin Dang[1,†], **Lei Bai**[2,†], **Jiazhen Dong**[2,†], **Xiaoping Hu**[3,†], **Jingchao Wang**[1], **Joao A. Paulo**[4], **Yan Xiong**[3], **Xiaowei Liang**[2], **Yishuang Sun**[5], **Yuncai Chen**[2], **Ming Guo**[2], **Xin Wang**[2], **Zhixiang Huang**[2], **Hiroyuki Inuzuka**[1], **Li Chen**[1], **Chen Chu**[6], **Jianping Liu**[7], **Tao Zhang**[1,‡], **Abdol-Hossein Rezaeian**[1], **Jing Liu**[1], **Husnu Ümit Kaniskan**[3], **Bo Zhong**[5,8], **Jinfang Zhang**[5,8], **Michael Letko**[9], **Jian Jin**[3,*], **Ke Lan**[2,5,8,*], **Wenyi Wei**[1,*]

[1]Department of Pathology, Beth Israel Deaconess Medical Center, Harvard Medical School, Boston, MA 02215, USA

[2]State Key Laboratory of Virology, College of Life Sciences, Wuhan University, Wuhan 430072, China

[3]Mount Sinai Center for Therapeutics Discovery, Departments of Pharmacological Sciences, Oncological Sciences and Neuroscience, Icahn School of Medicine at Mount Sinai, New York, NY 10029, USA

[4]Department of Cell Biology, Blavatnik Institute at Harvard Medical School, Boston, MA 02115, USA

[5]Medical Research Institute, Wuhan University, Wuhan 430071, China

[6]Department of Cancer Biology, Dana-Farber Cancer Institute and Department of Genetics, Blavatnik Institute, Harvard Medical School, Boston, MA 02215, USA

[7]State Key Laboratory of Bioorganic and Natural Products Chemistry, Center for Excellence in Molecular Synthesis, Shanghai Institute of Organic Chemistry, University of Chinese Academy of Sciences, Chinese Academy of Sciences, Shanghai 200032, China

[*]Corresponding author. jian.jin@mssm.edu (J.J.); klan@whu.edu.cn (K.L.); wwei2@bidmc.harvard.edu (W.W.).

[†]These authors contributed equally to this work.

[‡]Present address: Songjiang Research Institute, Songjiang Hospital, Shanghai Jiao Tong University School of Medicine, Shanghai 201600, China.

Author contributions: F.D. and W.W. conceived the project. F.D. performed the biochemistry and molecular biology-related works with help from J.W., H.I., L.C., T.Z., Jing Liu, and A.-H.R. L.B.and J.D. performed the authentic virus-related works with help from X.L., Y.C., M.G., X.W., and Z.H. X.H., Y.X., and H.U.K. designed and synthesized ML364 analogs. Y.S. performed the *Usp2*-KO mouse study, supervised by B.Z. and J.Z. C.C. performed the RNA-seq analysis. Jianping Liu performed the molecular docking analysis. J.A.P. performed the TMT-based proteomic analysis. M.L. assisted with the ACE2-dependent pseudotype entry assay. W.W., K.L., and J.J. supervised the study. F.D. wrote the manuscript with inputs from all co-authors. All authors commented on the manuscript.

Competing interests: W.W. is a co-founder and consultant for the Rekindle Therapeutics. J.J. is a cofounder and equity shareholder in Cullgen Inc., a scientific cofounder and scientific advisory board member of Onsero Therapeutics Inc., and a consultant for Cullgen Inc., EpiCypher Inc., Accent Therapeutics Inc., and Tavotek Biotherapeutics Inc. The Jin laboratory received research funds from Celgene Corporation, Levo Therapeutics Inc., Cullgen Inc., and Cullinan Oncology Inc. H.U.K. is a consultant for EpiCypher. A provisional patent application entitled “USP2 inhibitors and methods of using the same for the treatment of diseases” was filed and is pending. The inventors include J.J., W.W., W.G., Y.X., X.H., F.D., and J.Y. All other authors declare that they have no competing interests.

[8]TaiKang Center for Life and Medical Sciences, Wuhan University, Wuhan 430072, China

[9]Paul G. Allen School for Global Health, Washington State University, Pullman, WA 99163 USA

Abstract

Targeting angiotensin-converting enzyme 2 (ACE2) represents a promising and effective approach to combat not only the COVID-19 pandemic but also potential future pandemics arising from coronaviruses that depend on ACE2 for infection. Here, we report ubiquitin specific peptidase 2 (USP2) as a host-directed antiviral target; we further describe the development of MS102, an orally available USP2 inhibitor with viable antiviral activity against ACE2-dependent coronaviruses. Mechanistically, USP2 serves as a physiological deubiquitinase of ACE2, and targeted inhibition with specific small-molecule inhibitor ML364 leads to a marked and reversible reduction in ACE2 protein abundance, thereby blocking various ACE2-dependent coronaviruses tested. Using human ACE2 transgenic mouse models, we further demonstrate that ML364 efficiently controls disease caused by infection with severe acute respiratory syndrome coronavirus 2 (SARS-CoV-2), as evidenced by reduced viral loads and ameliorated lung inflammation. Furthermore, we improved the in vivo performance of ML364 in terms of both pharmacokinetics and antiviral activity. The resulting lead compound, MS102, holds promise as an oral therapeutic option for treating infections with coronaviruses that are reliant on ACE2.

INTRODUCTION

The severe acute respiratory syndrome coronavirus 2 (SARS-CoV-2) is a positive-sense single-stranded RNA virus, which is the root cause of the ongoing COVID-19 pandemic (1–3). Studies of the molecular mechanisms by which SARS-CoV-2 enters human cells revealed that the virus predominantly relies on the interaction of its surface spike (S) protein with the host cell receptor angiotensin-converting enzyme 2 (ACE2) (4–6). On the basis of these findings, multiple approaches have been developed to block SARS-CoV-2 infection by preventing S protein from binding to ACE2, including neutralizing antibodies (7–9) and ACE2-based binding peptide inhibitors (10, 11). In addition, multiple vaccines have been successfully developed and widely used, exhibiting great safety and efficacy in protecting against COVID-19 (12–15). Unfortunately, ongoing SARS-CoV-2 evolution across the viral genome, including changes in viral *S* gene, drives viral escape from immune surveillance and vaccination-elicited neutralizing antibodies (16–19), thereby rendering many existing COVID-19 therapeutics ineffective. Hence, it is imperative to prioritize the development of comprehensive and potent antiviral agents capable of combating SARS-CoV-2 and its emerging variants while remaining resilient against the ongoing viral evolution commonly observed in RNA viruses.

In this regard, substantial progress has been made in identifying small-molecule inhibitors that target the crucial enzymes involved in viral replication. For instance, N3 and ebselen, discovered through programmed screening of inhibitors targeting the main protease (M^{pro}, also known as the 3C-like protease or $3CL^{pro}$) of SARS-CoV-2, showed promising antiviral activity in cell-based assays (20). An oral SARS-CoV-2 M^{pro} inhibitor, nirmatrelvir, was shown to be effective for high-risk, nonhospitalized adults with COVID-19 (21). Inhibition

of the papain-like protease (PLpro) of SARS-CoV-2, another essential enzyme required for viral spread, with a small-molecule inhibitor, GRL0617, also suppressed SARS-CoV-2 infection and promoted antiviral immunity (22). In addition, remdesivir suppresses the viral RNA-dependent RNA polymerase and has demonstrated efficacy against SARS-CoV-2 when administered in accordance with appropriate clinical protocols (23, 24). Given the crucial role of S protein glycosylation in its interaction with ACE2, the inhibition of glycosylation through chemical inhibitors has emerged as a promising strategy to impede the entry of SARS-CoV-2 into host cells (25). Moreover, molnupiravir has demonstrated remarkable efficacy as an oral antiviral prodrug against SARS-CoV-2 (26). Nonetheless, apart from direct targeting of the RNA virus, it is theoretically postulated that drugs capable of eliminating the crucial host receptor required for viral entry, instead of inhibiting a viral protein or blocking viral-host interactions, could potentially diminish the likelihood of viral escape mutations. In this respect, small molecules targeting the androgen receptor (AR) and farnesoid X receptor (FXR), as well as the mammalian switch/sucrose non-fermentable (mSWI/SNF) chromatin remodeling complex, were reported to suppress *ACE2* transcription, thereby restricting SARS-CoV-2 infection (27–29). In the present study, we characterized the pivotal role of ubiquitin-specific peptidase 2 (USP2) as a physiological deubiquitinase of ACE2. Leveraging this finding, we have successfully developed an orally available small-molecule inhibitor that targets USP2, named MS102. This inhibitor induces transient degradation of ACE2 protein, resulting in inhibition of ACE2-dependent coronavirus infection.

RESULTS

USP2 serves as a physiological deubiquitinase of ACE2

Given the critical role of ACE2 in mediating infection with some coronaviruses (4, 30–33), elucidating how ACE2 is physiologically regulated could provide a broad therapeutic strategy against ACE2-dependent viral infections. In light of this, recent studies have identified AR, FXR, and the mSWI/SNF chromatin remodeling complex as key players in the transcriptional regulation of *ACE2* expression, and small-molecule inhibitors targeting these proteins were highlighted to be effective in restricting SARS-CoV-2 infection (27–29). However, the expression of both *AR* and *FXR* exhibits tissue and cell specificity (fig. S1, A and B), which could potentially limit the clinical efficacy of these therapies. In addition to the transcriptional control, posttranslational modifications also play an important role in regulating protein turnover. Thus, identifying the deubiquitinase of ACE2, which promotes protein survival in cells, could provide a viable approach for the purpose of blocking SARS-CoV-2 infection by reducing ACE2 protein abundance (Fig. 1A).

Before investigating ACE2 protein regulation, we performed validation of the ACE2 antibody by using short hairpin RNA (shRNA) technology to knockdown *ACE2* expression (fig. S1C). Given that intracellular proteins are mainly degraded by either the lysosome or proteasome pathways (34), we blocked gene translation using cycloheximide and treated HepG2 cells with chloroquine or MG132 to prevent lysosome- and proteasome-mediated proteolysis, respectively (fig. S1D). Using cyclin B1 and LC3B proteins as markers to assess the blockade of proteasome and lysosome functions, respectively, we found that

treatment of HepG2 cells with MG132, but not chloroquine, led to noticeable ACE2 protein accumulation (fig. S1E). These findings indicate that ACE2 undergoes proteasome-mediated degradation. In keeping with this notion, we were also able to detect K48-linked polyubiquitination on ACE2, which is a hallmark of proteins targeted for proteasomal degradation (fig. S1, F and G). In addition, we investigated the formation of linkage-specific ubiquitin chains on ACE2 and observed that ACE2 undergoes multiple forms of ubiquitination, including K6, K11, and K48 linkages (fig. S1H). To identify the lysine residue(s) serving as ubiquitination sites on ACE2, we generated a set of mutations against 13 residues. With these mutants, we observed a substantial reduction in ubiquitination signals upon mutation of the lysine residue K788 (fig. S1, I and J). The lysine residue K788 was reported previously to be ubiquitinated by the E3 ligase mouse double minute 2 (MDM2), involved in the regulation of ACE2 protein stability (35). Together, these results show that the ubiquitin-proteasome pathway plays an important role in mediating ACE2 protein degradation in cells.

Ubiquitination is a reversible process in which deubiquitinating enzymes (DUBs) play a crucial role by removing ubiquitin moieties from target proteins, thereby conferring protein stabilization (36). Thus, we established a HepG2 cell line expressing a fusion gene of *ACE2* and *Luciferase* (*ACE2-Luc*). With the utilization of this cell line, we conducted a screening for DUBs by using small interfering RNA (siRNA)–mediated gene knockdown (Fig. 1B). Among the DUBs screened, the silencing of *USP2* demonstrated the most notable reduction in ACE2-Luc signals (Fig. 1C). To validate this observation, we transfected HepG2 cells with four distinct siRNA oligos that specifically target *USP2*, which are different from the pool used in the initial screening. Consistently, ACE2-Luc signals were markedly reduced posttransfection of various siUSP2s (fig. S2, A and B). Furthermore, *USP2* silencing with siRNA led to a reduction in the abundance of endogenous ACE2 protein (Fig. 1D). To confirm the efficacy of USP2 inhibition, we used cyclin D1, a well-known USP2 substrate (37), as a positive control (Fig. 1D). Consistent findings were observed when using shRNA-mediated knockdown of *USP2*, further supporting the role of USP2 in ACE2 protein regulation (Fig. 1E and fig. S2C). Besides these cell culture models, we also observed a decrease in ACE2 protein abundance in spleen and kidney tissues derived from *Usp2*-null mice (fig. S2, D and E). In keeping with these findings, we found that ubiquitin-specific peptidase 2α (USP2α), the canonical isoform of USP2, physically interacted with ACE2 (Fig. 1F) and mediated its deubiquitination in vitro (Fig. 1, G and H, and fig. S2F). Moreover, the catalytic-inactive mutant of USP2α (C276A) failed to remove the ubiquitin moieties from ACE2 in cells (Fig. 1I and fig. S2G), confirming the critical role of USP2α in catalyzing deubiquitination of ACE2. In line with these observations, ectopic expression of USP2α prevented ACE2 protein degradation in HepG2 cells (fig. S2H).

To evaluate the hypothesis of blocking SARS-CoV-2 by down-regulating ACE2 through targeting USP2, we produced lentiviral luciferase reporter particles containing the S protein from SARS-CoV-2 (fig. S2I). First, we verified the incorporation of SARS-CoV-2 S protein into the particles produced following the protocol, as demonstrated by Western blot analysis (fig. S2J). Subsequently, we validated the reliance on ACE2 by the produced pseudotypes (fig. S2K). Using these pseudotyped viral particles, we observed decreases in pseudotype entry for SARS-CoV-2 wild-type (WT) and the Delta variant after siRNA-induced inhibition

of *USP2* (fig. S2, L to N). Furthermore, we observed a reduction in the entry of the authentic SARS-CoV-2 virus into Calu-3 cells (Fig. 1J). Together, these findings highlight a crucial role for USP2α in the modulation of ACE2 protein stability and its impact on SARS-CoV-2 infection.

USP2 inhibition with ML364 blocks ACE2-dependent coronavirus infection

In keeping with the findings that USP2 governs ACE2 deubiquitination and stabilization, treatment of HepG2 cells with USP2-specific inhibitor ML364 led to a reduction in the abundance of endogenous ACE2 protein and cytomegalovirus (CMV)–driven ACE2-Luc signals (Fig. 2A and fig. S3A). Furthermore, we observed that treatment with ML364 resulted in time- and dose-dependent reductions in ACE2 protein in multiple cell lines (Fig. 2B and fig. S3B). We observed a decrease in *ACE2* mRNA upon treatment with ML364 (fig. S3C). Nonetheless, we also noted a reduction in the abundance of ectopically expressed ACE2-Luc and CMV-driven ACE2 species in cells exposed to ML364 (Fig. 2C and fig. S3D). In addition, ML364 treatment inhibited USP2 activity and abolished USP2-mediated deubiquitination of ACE2 in vitro (fig. S3, E and F). Moreover, the ML364-induced reduction in ACE2 protein was largely reversed by MG132 treatment in HepG2 cells (fig. S3G). The addition of ML364, in comparison with cycloheximide single treatment, resulted in an accelerated degradation of ACE2 in both HepG2 and H1650 cells examined (Fig. 2D). Collectively, these findings suggest that USP2 inhibition with ML364 contributes to the reduction of ACE2 protein abundance, at least partially through posttranslational mechanisms.

Subcellular fractionation analysis revealed that membrane-bound ACE2 protein was decreased upon ML364 treatment (fig. S3H). Critically, ACE2 protein abundance was gradually recovered after the removal of ML364 from the medium (fig. S3I), suggesting that the ML364-induced ACE2 protein reduction is reversible. To understand the cellular protein profiles in response to ML364 treatment, we performed the tandem mass tag (TMT)–based quantitative proteomic analysis. Although we observed a substantial reduction in ACE2 protein through immunoblotting (fig. S3J), TMT–mass spectrometry analysis captured only one ACE2 peptide (data file S1). Nonetheless, we observed a significant ($P = 3.3 \times 10^{-6}$) decrease in cyclin D1 protein, providing support that the TMT results are reliable (fig. S3K). In keeping with the well-defined role of USP2 in cell cycle regulation (37), treatment with ML364 resulted in primarily cell cycle arrest (fig. S3, L and M). These findings provide further support for the reliability and validity of the TMT results. In line with the decreased abundance of ACE2 protein, we observed an obvious reduction in SARS-CoV-2 pseudovirus entry into cells in the context of ML364 treatment (Fig. 2E and fig. S4, A and B). ML364 treatment did not prevent the entry of non–ACE2-dependent pseudotypes, such as Middle East respiratory syndrome coronavirus (MERS-CoV) (fig. S4C), indicating that the antiviral effect of ML364 is likely ACE2 dependent. These results demonstrate that the cellular entry of SARS-CoV-2 can be effectively inhibited by targeting the ACE2 deubiquitinase USP2 using its specific small-molecule inhibitor ML364.

To compare the antiviral efficacy between targeting transcriptional regulation (AR and FXR) and posttranslational control (USP2) of ACE2, we identified three cell lines with

different *AR*, *FXR*, and *USP2* genotypes, AR^{+}/FXR^{+} (Calu-3), AR^{-}/FXR^{+} (HepG2), and AR^{+}/FXR^{-} (H1650) (fig. S4, D and E). Subsequently, we assessed the effectiveness of AR antagonist (ODM-201), FXR antagonist (ursodeoxycholic acid/UDCA and z-guggulsterone/ZGG), and USP2 inhibitor (ML364) in reducing ACE2 protein abundance in the three cell lines. USP2 inhibition led to reductions in ACE2 protein in all three cell lines examined, whereas the FXR antagonist UDCA only mildly reduced ACE2 protein in Calu-3 and HepG2, two *FXR*-positive cell lines (Fig. 2F and fig. S4F). AR antagonist ODM-201 also exhibited mild efficacy in reducing ACE2 protein in cells lacking *AR* at the concentrations tested, indicating the existence of mechanisms that are independent of AR (Fig. 2F and fig. S4F). Among these three cell lines, HepG2 cells were more sensitive to ML364 treatment, which may be because of its relatively higher *USP2* expression (fig. S4E). In line with the reduction in ACE2 protein, ML364 treatment prevented the pseudotype entry of SARS-CoV-2 in all cell lines examined, whereas UDCA and ZGG only showed mild effects when Calu-3 cells were pretreated for 48 hours (Fig. 2G and fig. S4G). In addition to SARS-CoV-2, ML364 treatment also exhibited promising activity against a panel of additional ACE2-dependent bat sarbecoviruses that are closely related to SARS-CoV-1 and SARS-CoV-2 (Fig. 2H). Therefore, these results support the conclusion that inhibition of USP2 using ML364 effectively mitigates ACE2-dependent viral infection by promoting the degradation of the ACE2 protein.

ACE2 is deubiquitinated by the SARS-CoV-2 PLpro

Given that SARS-CoV-2 PLpro shares a similar USP fold and conserved catalytic triad with USP2 (38), we wondered whether SARS-CoV-2 PLpro could functionally mimic USP2 to catalyze deubiquitination of ACE2. In line with the well-established role of SARS PLpro in governing deubiquitination of its substrate proteins (39), SARS-CoV-2 PLpro also displayed obvious deubiquitinase activity and the ability to deubiquitinate ACE2 in vitro (fig. S5, A and B). The PLpro proteins derived from SARS-CoV-1 and SARS-CoV-2, but not MERS-CoV, could promote deubiquitination of ACE2 in cells (fig. S5C). In further support of the notion that SARS-CoV-2 PLpro governs ACE2 deubiquitination, either disruption of the PLpro ubiquitin recognition domain or inactivation of its deubiquitinating activity by mutation of the active cysteine to serine (C111S) abolished its ability to remove ubiquitin moieties from ACE2 (fig. S5, D and E). Moreover, treatment of cells with the SARS-CoV-2 PLpro inhibitor GRL0617 diminished PLpro-induced ACE2 deubiquitination (fig. S5F). Together, these results demonstrate that SARS-CoV-2 PLpro serves as an upstream regulator of its viral receptor ACE2, mediating its deubiquitination.

Although SARS-CoV-2 PLpro displayed a similar role to USP2 in mediating the deubiquitination of ACE2, USP2 did not exhibit any activity toward the SARS-CoV-2 PLpro substrate, a small 5-nucleotide oligomer fluorogenic peptide, Z-RLRGG-AMC (fig. S5G). However, ML364 showed inhibitory effects against SARS-CoV-2 PLpro, as demonstrated in our experimental results (fig. S5H). In contrast, the well-established SARS-CoV-2 PLpro inhibitor GRL0617 exhibited no obvious activity toward USP2, even at a dose of 100 μM, in vitro (fig. S5I). To gain more insights into the inhibition of SARS-CoV-2 PLpro by ML364, we performed molecular docking analysis and found that ML364 could bind to the same pocket as GRL0617 on PLpro (fig. S5J). In support of this model, the presence of ML364

markedly reduced the inhibitory effect of GRL0617 on PLpro enzymatic activity (fig. S5K). These findings indicate that ML364 could competitively bind to PLpro with GRL0617. Thus, the overlap in target binding sites may impart ML364 with a dual antiviral strategy: blocking viral entry by mediating ACE2 degradation and simultaneously inhibiting viral replication by blocking PLpro processing of viral proteins.

To understand the differences in specificity among PLpro proteins derived from different coronaviruses in regulating ACE2 deubiquitination (fig. S5C), we conducted a sequence alignment analysis for these proteins. The ubiquitin recognition domain required for PLpro-mediated deubiquitination of ACE2 is conserved in the PLpro proteins derived from SARS-CoV-1 and SARS-CoV-2 but not in MERS-CoV (fig. S5L). This disparity explains the observed inability of MERS-CoV PLpro to deubiquitinate ACE2 in our experimental setting (fig. S5C). To test whether PLpro could influence the protein stability of ACE2 during SARS-CoV-2 infection, we examined the abundance of ACE2 protein in cells infected with SARS-CoV-2. We observed a reduction in ACE2 protein in SARS-CoV-2–infected cells (fig. S5M). Furthermore, treatment of cells with the PLpro inhibitor GRL0617 failed to prevent the infection-induced reduction of ACE2 (fig. S5M), indicating that the infection-induced reduction of ACE2 is likely independent of PLpro. Given that it was reported that the virus infection-induced ACE2 down-regulation is primarily accomplished through lysosomal degradation (40, 41), this may potentially represent a host-defensive mechanism aimed at preventing superinfection. This intriguing possibility warrants further exploration through additional research endeavors.

ML364 prevents infection with SARS-CoV-2 WT and variants in vitro

Next, we examined the kinetics of USP2 inhibition on ACE2 degradation and SARS-CoV-2 prevention. Using HepG2 as a representative model, we found that ACE2 protein abundance decreased by 50% within 12 hours of ML364 treatment (Fig. 3A). In addition, the inhibition of pseudotype entry is closely correlated to the degradation of ACE2, indicating that the inhibition of USP2 with ML364 hinders the entry of SARS-CoV-2 into cells in an ACE2-dependent manner (Fig. 3A). Moreover, we determined that the half-maximal inhibitory concentration (IC_{50}) value of ML364 against authentic SARS-CoV-2 in Calu-3 cells was approximately 4 μM (Fig. 3B). Furthermore, the application of ML364 to Calu-3 cells demonstrated an obvious reduction in the viral replication of the SARS-CoV-2 WT (Fig. 3C). Treatment of Calu-3 cells with ML364 led to broad inhibition of various authentic SARS-CoV-2 variants, including the Beta variant (Fig. 3D, and fig. S6, A to D) and the Delta variant (Fig. 3E, and fig. S7, A to D). In contrast, we did not observe any activity of ML364 against hCoV-OC43 (Fig. 3F), a human coronavirus that relies on 9-O-acetylated sialic acids for infection (42). These results demonstrate that the targeted inhibition of USP2 with ML364 effectively prevents the infection of ACE2-dependent SARS-CoV-2, irrespective of S protein mutations.

To determine a safe and suitable dosage of ML364 for administration in vivo, we performed pharmacokinetic measurements in male C57BL/6 mice. After a single intraperitoneal dose administration, the peak plasma concentration of ML364 was observed at 30 min, suggesting a rapid absorption and good exposure (Fig. 4A). On the basis of these data, we treated

male C57BL/6 mice with vehicle or ML364 (50 mg/kg, once a day or 35 mg/kg, twice a day) for 2 weeks. All animals were healthy without any clinical signs or deviation from baseline measurements being observed after the drug treatment. Moreover, in comparison to vehicle-treated animals, ML364 administration did not cause significant ($P = 0.86$) weight loss (fig. S8A). In considering the crucial roles of the ACE2-angiotensin-(1–7) pathway in maintaining normal cardiovascular function (43), we examined the plasma concentration of angiotensin-(1–7). The results showed that ML364 treatment did not lead to any noticeable reduction in angiotensin-(1–7) concentrations (fig. S8B). These findings imply that the regimens used were generally safe and well tolerated. In line with the observation that ML364 treatment promotes ACE2 degradation in cells, administration of C57BL/6 mice with ML364 also led to reduced abundance of ACE2 protein in several mouse tissues that we examined, including the pancreas, small intestine, and lung (fig. S8, C and D).

We then treated K18-hACE2 transgenic mice, which express human ACE2 driven by the human epithelial cell cytokeratin-18 (K18) promoter, with ML364 (50 mg/kg, daily administration) for a duration of 4 days, succeeded by a subsequent 6-day challenge with SARS-CoV-2 WT (Fig. 4B). The administration of ML364 to mice resulted in a reduction in the production of viral *E* and *N* genes in the lungs (Fig. 4C), as well as a significant ($P = 3.6 \times 10^{-6}$) decrease in viral loads (Fig. 4D). Consequently, hematoxylin and eosin (H&E) staining showed that the mice treated with ML364 had a reduction in overall lung pathology when compared with the animals treated with a control vehicle (Fig. 4E). To gain more insights into the mechanisms of protection conferred by ML364, we performed RNA sequencing (RNA-seq) analysis with the lung tissues harvested above. In comparison to the vehicle-treated mice, ML364 administration did not cause a broad range of gene expression changes in vivo, further indicating the safety of the treatment (Fig. 4F and fig. S8E). However, gene set enrichment analysis (GSEA) and Kyoto Encyclopedia of Genes and Genomes (KEGG) enrichment analysis showed that the inflammatory response signaling was down-regulated the most markedly in the lungs of ML364-treated mice (Fig. 4, G to I), which is consistent with the reduced viral load in ML364-treated mice. Moreover, the administration of ML364 significantly ($P = 0.01$) reduced the abundance of ACE2 protein in the lungs of these mice (fig. S8F). In summary, these results provide encouraging evidence for the feasibility of ML364 as a candidate for preventing SARS-CoV-2 infection.

Therapeutic administration of ML364 reduces SARS-CoV-2 viral load in vitro and in K18-hACE2 mice

To further evaluate the therapeutic potential for ML364 in the treatment of SARS-CoV-2 infection, we infected Calu-3 cells with authentic SARS-CoV-2 WT and several contemporary variants of concern for 1 hour before exposure to the PLpro inhibitor GRL0617, the USP2 inhibitor ML364, or a GRL0617-ML364 combination (Combo) for an additional 48 hours. ML364 alone or in combination with GRL0617 exhibited efficacy against all species of SARS-CoV-2 viruses tested, including WT, Beta variant, Delta variant, and Omicron BA.2 sublineage (Fig. 5, A and B). Furthermore, we tested these treatment regimens in vivo using the K18-hACE2 transgenic mouse model (Fig. 5C). Consistent with the findings observed in the cell culture model, the administration of ML364 at 6 hours after SARS-CoV-2 infection improved lung pathology when compared with the control group

treated solely with the vehicle (Fig. 5D). This was supported by a decrease in viral titers and in expression of the SARS-CoV-2 *E* gene in the lungs and small intestines of mice treated with ML364 (Fig. 5E and fig. S9A). In addition, we tested the above regimens for protection from Omicron BA.2 infection in vivo and observed similar results (fig. S9, B to D). Furthermore, we conducted a thorough investigation into the therapeutic effectiveness of ML364 for the treatment of SARS-CoV-2 infection using two additional hACE2 transgenic mouse models: C57BL/6-huACE2 (with ACE2 complete humanization, strain no. T037659) and C57BL/6-huACE2-Chimera (with ACE2 extracellular humanization, strain no. T037630). Our findings demonstrated that ML364 displayed substantial therapeutic potential in both mouse models (Fig. 5F and fig. S9, E to G). Together, these observations provide compelling evidence that ML364, by inhibiting USP2 and subsequently reducing ACE2 protein, effectively counteracts SARS-CoV-2 infection both in vitro and in vivo. These findings emphasize the potential of ML364 as a promising therapeutic candidate for combating SARS-CoV-2 irrespective of viral variations.

MS102 is an oral form of the USP2 inhibitor with improved pharmacokinetics and antiviral activity

Although ML364 showed promising therapeutic potential against ACE2-dependent viral infections, its existing pharmacokinetics prevented it from being a competitive clinical candidate (Fig. 4A). Thus, we explored ways to improve its pharmacokinetic properties while retaining or enhancing its antiviral efficacy by performing comprehensive chemical optimization. With this goal in mind, we designed and synthesized approximately 90 derivatives of ML364. By analyzing the abundance of cyclin D1 and ACE2 proteins after treatment with ML364 and its derivatives, one particular compound, termed MS102 (compound #56), emerged as the frontrunner (Fig. 6A and fig. S10, A to C). In comparison with ML364, MS102 features a bromo group added to the phenyl ring on the right, and the trifluoromethyl group at the central phenyl ring is relocated from the meta- to para-position of the sulfonamide moiety (fig. S10, D to F). Because ML364 treatment primarily led to cell cycle arrest (fig. S3L), we examined the cell viability after treatment with ML364 and its analogs. Once again, MS102 emerged as the top candidate based on the findings of this study (fig. S11A). In keeping with these results, MS102 exhibited slightly enhanced activity against USP2 (fig. S11B). To discern the differences between ML364 and MS102, we conducted a TMT-based proteomic analysis, revealing that both compounds exhibited similar protein reduction profiles (Fig. 6B and fig. S11C). In line with the enhanced capability to reduce ACE2 protein stability, MS102 demonstrated improved efficacy in blocking the infection of primary human bronchial epithelial (NHBE) cells by the authentic SARS-CoV-2 WT (Fig. 6C. The enhanced activity of MS102 was observed across all tested ACE2-dependent pseudotypes (Fig. 6D and fig. S11, D and E). Moreover, we evaluated the potential cell toxicity caused by ML364 or MS102 in HepG2 and Calu-3 cells used in our study. The results of measuring the LDH release in the context of ML364 or MS102 treatment showed that both compounds had minimal cytotoxicity (fig. S11F). Nonetheless, additional in-depth analyses are required to determine both the cytotoxicity of these compounds and any potential indirect impact they might have on SARS-CoV-2 infection.

Next, we conducted a comparative analysis of the antiviral efficacy between the approaches targeting transcriptional regulation of *ACE2* expression (e.g., FXR) and targeting the posttranslational control of ACE2 degradation (e.g., USP2). Although we observed a mild effect on ACE2-dependent pseudotype entry with FXR antagonist UDCA (Fig. 2G and fig. S11D), UDCA treatment exhibited efficacy in inhibiting the infection of Calu-3 cells by authentic SARS-CoV-2 (Fig. 6E and fig. S12A). Moreover, when comparing the three compounds, UDCA, ML364, and MS102, it is noteworthy that MS102 demonstrated superior activity against SARS-CoV-2 (Fig. 6E and fig. S12A). To verify the ACE2 dependency of USP2/FXR inhibition against viral infections, we conducted a cytopathic effect (CPE) assay using authentic hCoV-NL63 (an ACE2-dependent coronavirus) and hCoV-OC43 (an ACE2-independent viral strain). Our results showed that both ML364 and MS102 were effective in inhibiting the ACE2-dependent coronavirus hCoV-NL63, whereas they displayed limited or no activity against the ACE2-in-dependent strain hCoV-OC43, as observed at the evaluated concentrations (Fig. 6F and fig. S12, B and C). The FXR antagonist UDCA demonstrated no inhibitory activity against infections caused by either the hCoV-NL63 or the hCoV-OC43 viral strains (Fig. 6F and fig. S12, B and C). Meanwhile, remdesivir was evaluated in parallel and was active against both viral strains at the expected concentration, confirming the reliability of the assay (Fig. 6F and fig. S12, B and C). Collectively, these results confirmed the ACE2 dependency in the inhibition of USP2 by ML364 or MS102, thereby resulting in their inhibitory effects on viral infections. Moreover, these results indicate the presence of potential ACE2-independent mechanisms through which UDCA inhibits SARS-CoV-2 infection by targeting FXR inhibition, which warrants further investigations. In addition, it seems that a higher concentration of ML364 is required to inhibit infections of Calu-3 cells by SARS-CoV-2 (IC_{50} approximately 4 μM; Fig. 3B) as compared with hCoV-NL63 (IC_{50} approximately 0.18 μM; Fig. 6F). One possible explanation for this discrepancy could be attributed to the diversity in receptor utilization between the two viral strains. Although ACE2 is a receptor used by both SARS-CoV-2 and hCoV-NL63 to enter cells, SARS-CoV-2 has been reported to use some additional host receptors, such as Neuropilin-1 (44), CD147 (45), and TMEM106B (46). However, hCoV-NL63 likely does not use most of these alternative routes to infect cells, so reducing ACE2 abundance will strongly inhibit hCoV-NL63 infection, but SARS-CoV-2 might still find an alternative way to enter cells through other receptors.

Next, we investigated the in vivo pharmacokinetic properties of MS102 in C57BL/6 mice. MS102 showed a substantially higher peak plasma concentration, approximately threefold greater than that of ML364, and demonstrated remarkable improvement in stability, reaching concentrations approximately 2500 times greater than those of ML364 24 hours after administration (fig. S12D). The oral bioavailability of MS102 was unexpectedly found to be nearly 100%, highlighting its potential as an oral therapeutic candidate for future clinical applications (Fig. 6G). Furthermore, we evaluated the therapeutic efficacy of MS102 using the K18-hACE2 transgenic mouse model. In keeping with the findings observed in the cell culture models, MS102 displayed enhanced efficacy compared with ML364. This was evident from the enhanced reduction in the 50% tissue culture infectious dose ($TCID_{50}$) and improved lung pathology in the treated mice (fig. S12, E and F). Last, we assessed the effectiveness of ML364 and MS102 in promoting the survival of K18-hACE2 transgenic

mice after infection with SARS-CoV-2 Omicron BA.2 sublineage. The results demonstrated that the mice treated with MS102 exhibited notably enhanced outcomes compared with the control mice (Fig. 6H). Although we only observed a 3-day extension in MS102-treated mice compared with the vehicle-treated control group, the superior performance of MS102 over ML364 instills confidence in its potential as a candidate therapeutic agent. This outcome encourages us to explore and optimize the treatment regimens associated with MS102, thereby warranting comprehensive investigations in the future. In summary, these findings establish MS102 as an oral compound with improved antiviral activity, confirming that targeting posttranslational control of ACE2 through USP2 inhibition is a broad and effective therapeutic approach against ACE2-dependent coronaviruses (Fig. 6I).

DISCUSSION

The predominant reliance of SARS-CoV-2 and other coronaviruses on the host receptor ACE2 for cell entry makes ACE2 an attractive therapeutic target. Although multiple interventions have been developed to specifically disrupt SARS-CoV-2 S protein binding to ACE2 and thereby block viral infection (10, 11), identifying the endogenous modulators involved in the regulation of ACE2 protein stability is an alternative strategy to universally block different SARS-CoV-2 strains and other ACE2-dependent coronaviruses. In this respect, we identified USP2 as a physiological deubiquitinase of ACE2 and developed an oral USP2 inhibitor, MS102. In comparison with targeting transcriptional regulation of *ACE2* (e.g., through AR and FXR), direct efforts toward USP2 represent a more universal and effective approach for reducing the abundance of ACE2 protein and viral infections by ACE2-dependent coronaviruses (Figs. 2F and 6, E and F).

It is known that the PLpro of severe acute respiratory syndrome coronavirus (SARS-CoV) plays crucial roles in protecting the virus against host immune surveillance through removing ubiquitin and ISG15 conjugates from host proteins (22, 47). The SARS-CoV PLpro shares similar USP protein domain folding with human USP2, along with a conserved catalytic triad Cys-His-Asp (38). Given the structural similarity, in addition to ML364, several other USP2 inhibitors such as compound Z93 and thiopurine compounds 6MP and 6TG were also reported to inhibit SARS-CoV PLpro protease activity (38, 48, 49). As such, it would be feasible to design small-molecule inhibitors to dual-target USP2 and SARS-CoV PLpro, thereby blocking viral infection and replication simultaneously.

A number of viruses have been shown to exploit host cell cycle manipulation to facilitate their own replication (50, 51). For example, a recent study has highlighted the capability of SARS-CoV-2 to influence cell cycle checkpoints, leading to the arrest of host cells in G_2/M and S phases (52). Moreover, research has revealed the degradation of cyclin D1 and cyclin D3 in response to SARS-CoV-2 infection and revealed the role of cyclin D3 in restricting SARS-CoV-2 envelope incorporation into virions (53). In addition, it is intriguing to observe that elevated cyclin D1 promotes Epstein-Barr virus infection in nasopharyngeal epithelial cells (54). Thus, it is plausible to consider that disruptions in the cell cycle regulation caused by USP2 inhibition could substantially influence viral replication. Nonetheless, whether and how the ACE2-independent yet cell cycle–dependent impact of USP2 inhibition on viral replication warrants a more thorough and comprehensive investigation in the future.

In addition to serving as the entry point of SARS-CoV-1 and SARS-CoV-2, it is well known that ACE2 plays crucial roles in the renin-angiotensin system and is involved in many human diseases, including hypertension, diabetes, and cardiovascular disease (55). Although additional studies are required to assess the safety of modulating the ACE2 system, results from studies in mice lacking the *Ace2* gene have shown that these animals are healthy, fertile, and exhibit no abnormal cardiac characteristics (56). Moreover, mice with *Usp2* deficiency are able to survive (57, 58), and our in vivo studies have revealed that there is no substantial change in angiotensin-(1–7) concentrations after a short period of treatment with ML364 (fig. S8B). In addition, our RNA-seq analyses did not indicate any substantial alterations in the expression of genes linked to cardiovascular disease after ML364 treatment (Fig. 4F and fig. S8E). The US Food and Drug Administration–approved FXR antagonist UDCAwas recently revealed to be able to protect from SARS-CoV-2 infection by reducing *ACE2* expression at the transcriptional level (28), demonstrating the safety and practicality of temporarily reducing ACE2 protein abundance.

Our study has several limitations. First, we used human ACE2 transgenic mouse models to evaluate the therapeutic potential of USP2 inhibitors in preventing SARS-CoV-2 infection. Given that our strategy is aimed at preventing virus entry by down-regulating the abundance of ACE2 protein through targeting its deubiquitinase USP2, the mouse models we used have very high *ACE2* expression and therefore may potentially mask real protective effects. Thus, it is imperative to extend our investigations to encompass more physiologically relevant in vivo models to obtain more human-relevant phenotypes. In addition, USP2 inhibition primarily led to cell cycle arrest, and numerous viruses exploit the host cell cycle machinery to support their replication. Gaining a comprehensive understanding of the interplay between USP2 inhibition-induced cell cycle arrest and viral replication is essential to elucidate the broader implications. Moreover, although we observed a reduction in *ACE2* mRNA expressions after treatment with USP2 inhibitor (fig. S3C), we refrained from delving extensively into exploring this avenue. Investigating the potential mechanisms underlying the observed reduction in *ACE2* mRNA remains an unexplored facet that could introduce an additional mechanism contributing to the overall phenotype. Last, although the compound MS102 developed in this study is based on the well-established USP2 inhibitor ML364, a critical step in understanding its mechanism of action and confirming its on-target efficacy necessitates the determination of the USP2-MS102 co-crystal structure.

In conclusion, the discoveries of this research elucidate a physiological function of the USP2 deubiquitinase in governing the deubiquitination process of ACE2, consequently playing a role in maintaining its protein stability. Moreover, this study provides evidence for the viability of preventing ACE2-dependent coronavirus infections by inhibiting USP2 deubiquitinase. Furthermore, we have successfully developed an orally bioavailable USP2 inhibitor, MS102. These findings offer a promising oral therapeutic option for treating viral infections that depend on ACE2.

MATERIALS AND METHODS

Study design

The primary objective of this study was to investigate the mechanisms underlying ACE2 protein stability regulation and its implications in preventing ACE2-dependent coronavirus infections. To this end, we initiated a comprehensive investigation using siRNA-based deubiquitinase screening, which led to the identification of USP2 as a key deubiquitinase responsible for ACE2 modulation. Subsequently, our efforts were directed toward unraveling the mechanisms through which USP2 exerts its regulatory influence on ACE2. Concurrently, we aimed to validate the viability of USP2-based therapeutic approaches for the prevention of SARS-CoV-2 infection. This encompassed a multifaceted approach involving in vitro cell culture experiments and in vivo assessments using mouse models. Furthermore, we attempted to optimize the USP2 inhibitor ML364 to enhance its stability. Our endeavors culminated in the development of an oral formulation of the USP2 inhibitor MS102. In our experimental design, animals were randomized into distinct groups, with treatments being administered according to the predefined criteria. Animals displaying abnormal or unhealthy conditions were excluded before the start of the study. Experiments were stopped, and tissues were harvested when the vehicle-treated mice had serious clinical signs but were still alive. Throughout the course of this study, each experiment involved a minimum of four mice per group, and all experiments were performed at least twice unless otherwise indicated in the figure legends.

Animals

C57BL/6 male mice (Taconic Biosciences) were used for evaluating the effect of ML364 on promoting ACE2 degradation in vivo. The study was approved by the Beth Israel Deaconess Medical Center Institutional Animal Care and Use Committee (IACUC; protocol number 019-2021) and performed in accordance with guidelines established by the National Institutes of Health Guide for the Care and Use of Laboratory Animals. *Usp2*-null mice have a C57BL/6 background, as described previously (57, 58). For the in vivo SARS-CoV-2 challenge study, K18-hACE2 transgenic mice (strain no. T037657), C75BL/6-HuACE2 transgenic mice (strain no. T037659), and C75BL/6-HuACE2-Chimera mice (strain no. T037630) were purchased from Gempharmatech Co. Ltd. All authentic viral studies were approved by the Animal Care and Use Committee of Wuhan University (protocol number WP20210527) and were performed in the animal biosafety level 3 laboratory at Wuhan University. For drug metabolism and pharmacokinetic determination, the service was provided by Sai Life Sciences Limited (India). All animals were housed on a 12-light/12-dark cycle, a temperature of 70° ± 5 F, and humidity of 40 to 60%.

Cell lines and cell culture

All cells were cultured in a humidified atmosphere at 37°C and 5% CO_2. The investigation primarily involved HepG2, Calu-3, H1650, Vero E6, NHBE, Huh7, LLC-MK2, and BHK21 cell lines. In addition, a range of cell lines was used to examine the expression status of ACE2. Vero E6, HepG2, human embryonic kidney (HEK) 293T, Huh7, MDA-MB-468, MDA-MB-157, and CAMA-1 cells were purchased from ATCC (American Type Culture Collection) and were cultured in Dulbecco’s modified Eagle’s medium (DMEM). DLD-1,

A549, H2228, H1975, H1299, H157, H1650, HCC38, HCC1143, HCC1806, BT-549, AU565, ZR-75-30, BT-474, HCC1569, ZR-75-1, and HCC1428 cells were purchased from ATCC and were cultured in RPMI 1640 medium. LIM2405, RKO, DiFi, SW480, LIM1215, LoVo, LS411N, SW1463, SW48, SNU-C2B, HCT-8, and SW837 cells were obtained from L. Zhang's lab at the University of Pittsburgh and were cultured in RPMI 1640 medium. The Calu-3 cell line was from the P. Liu lab at University of North Carolina at Chapel Hill and cultured in DMEM. 16HBE14o- and Beas-2B cells were from the X. Zhou lab at Brigham and Women's Hospital and cultured in DMEM. 786-O and RCC4 cell lines were obtained from Z. Ding's lab at the University of Texas MD Anderson Cancer Center and cultured in DMEM. LLC-MK2 and BHK21 cells were maintained by the service provider, ImQuest BioSciences Inc. NHBE cells were purchased from ATCC and were maintained in airway epithelial cell basal medium (ATCC, PCS-300-030) supplemented with the Bronchial/Tracheal Epithelial Cell Growth Kit (ATCC, PCS-300-040). All cell culture media were supplemented with 10% fetal bovine serum (10437028, Gibco) and 1% penicillin/streptomycin (151401122, Gibco).

Plasmids and reagents

ACE2 cDNA ORF clone (HG10108-CF), TMPRSS2 cDNA ORF clone (HG13070), SARS-CoV-2 NSP3 gene ORF cDNA clone (VG40593-UT), SARS coronavirus (strain WH20) PLpro gene ORF cDNA clone (VG40524-CF), and MERS-CoV PLpro gene ORF cDNA clone (VG40522-CF) were purchased from Sino Biological US Inc. S protein pseudotyping plasmids of Delta variant (B.1.617.2), Alpha variant (B.1.1.7), Beta variant (B.1.351), Gamma variant (P.1), and Omicron BA.1 (B.1.1.529) were purchased from InvivoGen. pMD2.G (#12259), psPAX2 (#12260), and pLenti-CMV-GFP (#17448) were purchased from Addgene. shRNA bacterial clone oligos against *ACE2* (TRCN0000046693, TRCN0000046694, and TRCN0000046695) and *USP2* (TRCN0000007277, TRCN0000007278, and TRCN0000011080) were purchased from Sigma-Aldrich Inc. The FlexiTube siRNA molecules against Human USP2 were purchased from Qiagen (catalog no. 1027416). Myc-tagged USP2α WT and C276A constructs were gifts from W. Gu's lab at Columbia University Irving Medical Center. pCG1-SARS-2-S-HA plasmid was a gift from S. Poöhlmann's lab at German Primate Center, Germany. S protein pseudotyping plasmids of MERS, SARS-CoV-1, WIV1, SHC014, Rs4231, Rs4084, LYRa11, Rs7327, hCoV-229E, and Khosta-2 were provided by M. Letko at Washington State University. Other constructs and mutations were generated in this study, and the cloning primers are provided in table S1. All these homemade constructs were validated by Sanger sequencing. MG-132 (S2619), chloroquine (S6999), and cycloheximide (S7418) were purchased from Selleckchem. DUB inhibitors used in this study were purchased from MedChemExpress.

Statistics and reproducibility

All raw, individual-level data are presented in data file S2. All data shown are representative of two or more independent experiments with similar results unless specified otherwise in the figure legends. Statistical analyses were performed as defined in the figure legends, and results are represented as mean ± SEM unless otherwise noted. The sample size (n) refers to the number of independent biological samples tested. Differences were considered

statistically significant at $P \leq 0.05$. No statistical methods were used to predetermine the sample size.

Supplementary Material

Refer to Web version on PubMed Central for supplementary material.

Acknowledgments:

We thank all members of the Wei Lab for critical reading and thoughtful comments on the manuscript.

Funding:

This work is supported by 1K99CA263194 (to F.D.), R35CA253027 (to W.W.), and grants (32188101 and 81930060) from the Natural Science Foundation of China (to K.L.). This work used the tandem mass spectrometry system at Harvard Medical School with funding from NIH grant R01GM132129 (to J.A.P.).

Data and materials availability:

All data associated with this study are present in the paper or the Supplementary Materials. The RNA-seq data generated in this study have been deposited into the Gene Expression Omnibus Database with the accession number GSE237741. Reagents generated in this study are available upon reasonable request accompanied by material transfer agreement through reaching out to W.W.

REFERENCES AND NOTES

1. Chen L, Liu W, Zhang Q, Xu K, Ye G, Wu W, Sun Z, Liu F, Wu K, Zhong B, Mei Y, Zhang W, Chen Y, Li Y, Shi M, Lan K, Liu Y, RNA based mNGS approach identifies a novel human coronavirus from two individual pneumonia cases in 2019 Wuhan outbreak. Emerg. Microbes infect 9, 313–319 (2020). [PubMed: 32020836]
2. Zhou P, Yang XL, Wang XG, Hu B, Zhang L, Zhang W, Si HR, Zhu Y, Li B, Huang CL, Chen HD, Chen J, Luo Y, Guo H, Jiang RD, Liu MQ, Chen Y, Shen XR, Wang X, Zheng XS, Zhao K, Chen QJ, Deng F, Liu LL, Yan B, Zhan FX, Wang YY, Xiao GF, Shi ZL, A pneumonia outbreak associated with a new coronavirus of probable bat origin. Nature 579, 270–273 (2020). [PubMed: 32015507]
3. Zhu N, Zhang D, Wang W, Li X, Yang B, Song J, Zhao X, Huang B, Shi W, Lu R, Niu P, Zhan F, Ma X, Wang D, Xu W, Wu G, Gao GF, Tan W; China Novel Coronavirus Investigating and Research Team, A Novel Coronavirus from Patients with Pneumonia in China, 2019. N. Engl. J. Med 382, 727–733 (2020). [PubMed: 31978945]
4. Hoffmann M, Kleine-Weber H, Schroeder S, Kruger N, Herrler T, Erichsen S, Schiergens TS, Herrler G, Wu NH, Nitsche A, Muller MA, Drosten C, Pohlmann S, SARS-CoV-2 cell entry depends on ACE2 and TMPRSS2 and is blocked by a clinically proven protease inhibitor. Cell 181, 271–280.e8 (2020). [PubMed: 32142651]
5. Letko M, Marzi A, Munster V, Functional assessment of cell entry and receptor usage for SARS-CoV-2 and other lineage B betacoronaviruses. Nat. Microbiol 5, 562–569 (2020). [PubMed: 32094589]
6. Yan R, Zhang Y, Li Y, Xia L, Guo Y, Zhou Q, Structural basis for the recognition of SARS-CoV-2 by full-length human ACE2. Science 367, 1444–1448 (2020). [PubMed: 32132184]
7. Chi X, Yan R, Zhang J, Zhang G, Zhang Y, Hao M, Zhang Z, Fan P, Dong Y, Yang Y, Chen Z, Guo Y, Zhang J, Li Y, Song X, Chen Y, Xia L, Fu L, Hou L, Xu J, Yu C, Li J, Zhou Q, Chen W, A neutralizing human antibody binds to the N-terminal domain of the Spike protein of SARS-CoV-2. Science 369, 650–655(2020). [PubMed: 32571838]

8. Rogers TF, Zhao F, Huang D, Beutier N, Burns A, He WT, Limbo O, Smith C, Song G, Woehi J, Yang L, Abbott RK, Callaghan S, Garcia E, Hurtado J, Parren M, Peng L, Ramirez S, Ricketts J, Ricciardi MJ, Rawlings SA, Wu NC, Yuan M, Smith DM, Nemazee D, Teijaro JR, Voss JE, Wilson IA, Andrabi R, Briney B, Landais E, Sok D, Jardine JG, Burton DR, Isolation of potent SARS-CoV-2 neutralizing antibodies and protection from disease in a small animal model. Science 369, 956–963 (2020). [PubMed: 32540903]

9. Wu Y, Wang F, Shen C, Peng W, Li D, Zhao C, Li Z, Li S, Bi Y, Yang Y, Gong Y, Xiao H, Fan Z, Tan S, Wu G, Tan W, Lu X, Fan C, Wang Q, Liu Y, Zhang C, Qi J, Gao GF, Gao F, Liu L, A noncompeting pair of human neutralizing antibodies block COVID-19 virus binding to its receptor ACE2. Science 368, 1274–1278 (2020). [PubMed: 32404477]

10. Cao L, Goreshnik I, Coventry B, Case JB, Miller L, Kozodoy L, Chen RE, Carter L, Walls AC, Park YJ, Strauch EM, Stewart L, Diamond MS, Veesler D, Baker D, De novo design of picomolar SARS-CoV-2 miniprotein inhibitors. Science 370, 426–431 (2020). [PubMed: 32907861]

11. Han Y, Krai P, Computational Design of ACE2-Based Peptide Inhibitors of SARS-CoV-2. ACS Nano 14, 5143–5147 (2020). [PubMed: 32286790]

12. Polack FP, Thomas SJ, Kitchin N, Absalon J, Gurtman A, Lockhart S, Perez JL, Marc GP, Moreira ED, Zerbini C, Bailey R, Swanson KA, Roychoudhury S, Koury K, Li P, Kalina WV, Cooper D, Frenck RW Jr, Hammitt LL, Türeci Ö, Nell H, Schaefer A, ünal S, Tresnan DB, Mather S, Dormitzer PR, Ćahin U, Jansen KU, Gruber WC; C4591001 Clinical Trial Group, Safety and Efficacy of the BNT162b2 mRNA Covid-19 Vaccine. N. Engl. J. Med 383, 2603–2615 (2020). [PubMed: 33301246]

13. Baden LR, El Sahly HM, Essink B, Kotloff K, Frey S, Novak R, Diemert D, Spector SA, Rouphael N, Creech CB, McGettigan J, Khetan S, Segall N, Solis J, Brosz A, Fierro C, Schwartz H, Neuzil K, Corey L, Gilbert P, Janes H, Follmann D, Marovich M, Mascola J, Polakowski L, Ledgerwood J, Graham BS, Bennett H, Pajon R, Knightly C, Leav B, Deng W, Zhou H, Han S, Ivarsson M, Miller J, Zaks T; COVE Study Group, Efficacy and Safety of the mRNA-1273 SARS-CoV-2 Vaccine. N. Engl. J. Med 384, 403–416 (2021). [PubMed: 33378609]

14. Sadoff J, Gray G, Vandebosch A, Cardenas V, Shukarev G, Grinsztejn B, Goepfert PA, Truyers C, Fennema H, Spiessens B, Offergeld K, Scheper G, Taylor KL, Robb ML, Treanor J, Barouch DH, Stoddard J, Ryser MF, Marovich MA, Neuzil KM, Corey L, Cauwenberghs N, Tanner T, Hardt K, Ruiz-Guinazu J, Le Gars M, Schuitemaker H, Van Hoof J, Struyf F, Douoguih M; ENSEMBLE Study Group, Safety and efficacy of single-dose Ad26.COV2.S vaccine against Covid-19. N. Engl. J. Med 384, 2187–2201 (2021). [PubMed: 33882225]

15. Xia S, Zhang Y, Wang Y, Wang H, Yang Y, Gao GF, Tan W, Wu G,Xu M, Lou Z, Huang W, Xu W, Huang B, Wang H, Wang W, Zhang W, Li N, Xie Z, Ding L, You W, Zhao Y, Yang X, Liu Y,Wang Q,Huang L,Yang Y,Xu G,Luo B, Wang W,Liu P, Guo W,Yang X, Safety and immunogenicity of an inactivated SARS-CoV-2 vaccine, BBIBP-CorV: A randomised, doubleblind, placebo-controlled, phase 1/2 trial. Lancet Infect. Dis 21, 39–51 (2021). [PubMed: 33069281]

16. Hoffmann M, Arora P, Gross R, Seidel A, Hornich BF, Hahn AS, Kruger N, Graichen L, Hofmann-Winkler H, Kempf A, Winkler MS, Schulz S, Jack HM, Jahrsdorfer B, Schrezenmeier H,Muller M, Kleger A,Munch J,Pohlmann S, SARS-CoV-2 variants B.1.351 and P.1 escape from neutralizing antibodies. Cell 184, 2384–2393.e12 (2021). [PubMed: 33794143]

17. Mlcochova P, Kemp SA, Dhar MS, Papa G, Meng B, Ferreira IATM, Datir R, Collier DA, Albecka A, Singh S, Pandey R, Brown J, Zhou J, Goonawardane N, Mishra S, Whittaker C, Mellan T, Marwal R, Datta M, Sengupta S, Ponnusamy K, Radhakrishnan VS, Abdullahi A, Charles O, Chattopadhyay P, Devi P, Caputo D, Peacock T, Wattal C, Goel N, Satwik A, Vaishya R, Agarwal M; Indian SARS-CoV-2 Genomics Consortium (INSACOG); Genotype to Phenotype Japan (G2P-Japan) Consortium; CITIID-NIHR BioResource COVID-19 Collaboration, Mavousian A, Lee JH, Bassi J, Silacci-Fegni C, Saliba C, Pinto D, Irie T, Yoshida I, Hamilton WL, Sato K, Bhatt S, Flaxman S, James LC, Corti D, Piccoli L, Barclay WS, Rakshit P, Agrawal A, Gupta RK, SARS-CoV-2 B.1.617.2 Delta variant replication and immune evasion. Nature 599, 114–119 (2021). [PubMed: 34488225]

18. Cao Y, Wang J, Jian F, Xiao T, Song W, Yisimayi A, Huang W, Li Q, Wang P, An R, Wang J, Wang Y, Niu X, Yang S, Liang H, Sun H, Li T, Yu Y, Cui Q, Liu S, Yang X, Du S, Zhang Z, Hao X, Shao F, Jin R, Wang X, Xiao J, Wang Y, Xie XS, Omicron escapes the majority of existing SARS-CoV-2 neutralizing antibodies. Nature 602, 657–663 (2022). [PubMed: 35016194]

19. Chen Y, Liu Q, Zhou L, Zhou Y, Yan H, Lan K, Emerging SARS-CoV-2 variants: Why, how, and what's next? Cell Insight 1, 100029(2022). [PubMed: 37193049]

20. Jin Z, Du X, Xu Y, Deng Y, Liu M, Zhao Y, Zhang B, Li X, Zhang L, Peng C, Duan Y, Yu J, Wang L, Yang K, Liu F, Jiang R, Yang X, You T, Liu X, Yang X, Bai F, Liu H, Liu X, Guddat LW, Xu W, Xiao G, Qin C,Shi Z, Jiang H, Rao Z, Yang H, Structure of Mpro from SARS-CoV-2 and discovery of its inhibitors. Nature 582, 289–293 (2020). [PubMed: 32272481]

21. Hammond J, Leister-Tebbe H, Gardner A, Abreu P, Bao W, Wisemandle W, Baniecki M, Hendrick VM, Damle B, Simon-Campos A, Pypstra R, Rusnak JM; EPIC-HR Investigators, Oral Nirmatrelvir for High-Risk, Nonhospitalized Adults with Covid-19. N. Engl. J. Med 386, 1397–1408 (2022). [PubMed: 35172054]

22. Shin D, Mukherjee R, Grewe D, Bojkova D, Baek K, Bhattacharya A, Schulz L, Widera M, Mehdipour AR, Tascher G, Geurink PP, Wilhelm A, van der Heden van Noort GJ, Ovaa H, Müller S, Knobeloch K-P, Rajalingam K, Schulman BA, Cinatl J, Hummer G, Ciesek S, Dikic I, Papain-like protease regulates SARS-CoV-2 viral spread and innate immunity. Nature 587, 657–662 (2020). [PubMed: 32726803]

23. Beigel JH, Tomashek KM, Dodd LE, Mehta AK, Zingman BS, Kalil AC, Hohmann E, Chu HY, Luetkemeyer A, Kline S, Lopez de Castilla D, Finberg RW, Dierberg K, Tapson V, Hsieh L, Patterson TF, Paredes R, Sweeney DA, Short WR, Touloumi G, Lye DC, Ohmagari N, Oh MD, Ruiz-Palacios GM, Benfield T, Fatkenheuer G, Kortepeter MG, Atmar RL, Creech CB, Lundgren J, Babiker AG, Pett S, Neaton JD, Burgess TH, Bonnett T, Green M, Makowski M, Osinusi A, Nayak S, Lane HC; ACTT-1 Study Group Members, Remdesivir for the treatment of Covid-19 - Final report. N. Engl. J. Med 383, 1813–1826 (2020). [PubMed: 32445440]

24. Gordon CJ, Tchesnokov EP, Woolner E, Perry JK, Feng JY, Porter DP, Gotte M, Remdesivir is a direct-acting antiviral that inhibits RNA-dependent RNA polymerase from severe acute respiratory syndrome coronavirus 2 with high potency. J. Biol. Chem 295, 6785–6797 (2020). [PubMed: 32284326]

25. Yang Q, Hughes TA, Kelkar A, Yu X, Cheng K, Park S, Huang WC, Lovell JF, Neelamegham S, Inhibition of SARS-CoV-2 viral entry upon blocking N- and O-glycan elaboration. eLife 9, (2020).

26. Bernal AJ, da Silva MMG, Musungaie DB, Kovalchuk E, Gonzalez A, Reyes VD, Martin-Quiros A, Caraco Y, Williams-Diaz A, Brown ML, Du J, Pedley A, Assaid C, Strizki J, Grobler JA, Shamsuddin HH, Tipping R, Wan H, Paschke A, Butterton JR, Johnson MG, De Anda C; MOVe-OUT Study Group, Molnupiravir for oral treatment of Covid-19 in nonhospitalized patients. N. Engl. J. Med 386, 509–520 (2022). [PubMed: 34914868]

27. Qiao Y, Wang X-M, Mannan R, Pitchiaya S, Zhang Y, Wotring JW, Xiao L, Robinson DR, Wu Y-M, Tien JC-Y, Cao X, Simko SA, Apel IJ, Bawa P, Kregel S, Narayanan SP, Raskind G, Ellison SJ, Parolia A, Zelenka-Wang S, McMurry L, Su F, Wang R, Cheng Y, Delekta AD, Mei Z, Pretto CD, Wang S, Mehra R, Sexton JZ, Chinnaiyan AM, Targeting transcriptional regulation of SARS-CoV-2 entry factors *ACE2* and *TMPRSS2*.Proc. Natl. Acad. Sci. U.S.A 118, e2021450118 (2021). [PubMed: 33310900]

28. Brevini T, Maes M, Webb GJ, John BV, Fuchs CD, Buescher G, Wang L, Griffiths C, Brown ML, Scott WE 3rd, Pereyra-Gerber P, Gelson WTH, Brown S, Dillon S, Muraro D, Sharp J, Neary M, Box H, Tatham L, Stewart J, Curley P, Pertinez H, Forrest S, Mlcochova P, Varankar SS, Darvish-Damavandi M, Mulcahy VL, Kuc RE, Williams TL, Heslop JA, Rossetti D, Tysoe OC, Galanakis V, Vila-Gonzalez M, Crozier TWM, Bargehr J, Sinha S, Upponi SS, Fear C, Swift L, Saeb-Parsy K, Davies SE, Wester A, Hagstrom H, Melum E, Clements D, Humphreys P, Herriott J, Kijak E, Cox H,Bramwell C, Valentijn A, Illingworth CJR; Consortium UK-PBC, Dahman B, Bastaich DR, Ferreira RD, Marjot T, Barnes E, Moon AM, Barritt AS 4th, Gupta RK, Baker S, Davenport AP, Corbett G, Gorgoulis VG, Buczacki SJA, Lee J-H, Matheson NJ, Trauner M, Fisher AJ, Gibbs P, Butler AJ, Watson CJE, Mells GF, Dougan G, Owen A, Lohse AW, Vallier L, Sampaziotis F, FXR inhibition may protect from SARS-CoV-2 infection by reducing ACE2. Nature 615, 134–142 (2022). [PubMed: 36470304]

29. Wei J, Patil A, Collings CK, Alfajaro MM, Liang Y, Cai WL, Strine MS, Filler RB, DeWeirdt PC, Hanna RE, Menasche BL, Okten A, Pena-Hernandez MA, Klein J, McNamara A, Rosales R, McGovern BL, Luis Rodriguez M, Garcia-Sastre A, White KM, Qin Y, Doench JG, Yan Q, Iwasaki A, Zwaka TP, Qi J, Kadoch C, Wilen CB, Pharmacological disruption of mSWI/SNF

complex activity restricts SARS-CoV-2 infection. Nat. Genet 55, 471–483 (2023). [PubMed: 36894709]

30. Li W, Moore MJ, Vasilieva N, Sui J, Wong SK, Berne MA, Somasundaran M, Sullivan JL, Luzuriaga K, Greenough TC, Choe H, Farzan M, Angiotensin-converting enzyme 2 is a functional receptor for the SARS coronavirus. Nature 426, 450–454 (2003). [PubMed: 14647384]
31. Hofmann H, Pyrc K, van der Hoek L, Geier M, Berkhout B, Pohlmann S, Human coronavirus NL63 employs the severe acute respiratory syndrome coronavirus receptor for cellular entry. Proc. Natl. Acad. Sci. U.S.A 102, 7988–7993 (2005). [PubMed: 15897467]
32. Seifert SN, Bai S, Fawcett S, Norton EB, Zwezdaryk KJ, Robinson J, Gunn B, Letko M, An ACE2-dependent Sarbecovirus in Russian bats is resistant to SARS-CoV-2 vaccines. PLOS Pathog. 18, el010828 (2022).
33. Xiong Q, Cao L, Ma C, Tortorici MA, Liu C, Si J, Liu P, Gu M, Walls AC, Wang C, Shi L, Tong F, Huang M, Li J, Zhao C, Shen C, Chen Y, Zhao H, Lan K, Corti D, Veesler D, X Wang H Yan, Close relatives of MERS-CoV in bats use ACE2 as their functional receptors. Nature 612, 748–757 (2022). [PubMed: 36477529]
34. Ciechanover A, Proteolysis: From the lysosome to ubiquitin and the proteasome. Nat. Rev. Mol. Cell Biol 6, 79–87 (2005). [PubMed: 15688069]
35. Shen H, Zhang J, Wang C, Jain PP, Xiong M, Shi X, Lei Y, Chen S, Yin Q, Thistlethwaite PA, Wang J, Gong K, Yuan ZY, Yuan JX, Shyy JY, MDM2-mediated ubiquitination of angiotensin-converting enzyme 2 contributes to the development of pulmonary arterial hypertension. Circulation 142, 1190–1204 (2020). [PubMed: 32755395]
36. Reyes-Turcu FE, Ventii KH, Wilkinson KD, Regulation and cellular roles of ubiquitin-specific deubiquitinating enzymes. Annu. Rev. Biochem 78, 363–397 (2009). [PubMed: 19489724]
37. Shan J, Zhao W, Gu W, Suppression of cancer cell growth by promoting cyclin D1 degradation. Mol. Cell 36, 469–476 (2009). [PubMed: 19917254]
38. Mirza MU, Ahmad S, Abdullah I, Froeyen M, Identification of novel human USP2 inhibitor and its putative role in treatment of COVID-19 by inhibiting SARS-CoV-2 papain-like (PLpro) protease. Comput. Biol. Chem 89, 107376 (2020). [PubMed: 32979815]
39. Békés M, Rut W, Kasperkiewicz P, Mulder MP, Ovaa H, Drag M, Lima CD, Huang TT, SARS hCoV papain-like protease is a unique Lys48 linkage-specific di-distributive deubiquitinating enzyme. Biochem. J 468, 215–226 (2015). [PubMed: 25764917]
40. Kuba K, Imai Y, Rao S, Gao H, Guo F, Guan B, Huan Y, Yang P, Zhang Y, Deng W, Bao L, Zhang B, Liu G, Wang Z, Chappell M, Liu Y, Zheng D, Leibbrandt A, Wada T, Slutsky AS, Liu D, Qin C, Jiang C, Penninger JM, A crucial role of angiotensin converting enzyme 2 (ACE2) in SARS coronavirus-induced lung injury. Nat. Med 11, 875–879 (2005). [PubMed: 16007097]
41. Lu Y, Zhu Q, Fox DM, Gao C, Stanley SA, Luo K, SARS-CoV-2 down-regulates ACE2 through lysosomal degradation. Mol. Biol. Cell 33, ar147 (2022). [PubMed: 36287912]
42. Hulswit RJG, Lang Y, Bakkers MJG, Li W, Li Z, Schouten A, Ophorst B, van Kuppeveld FJM, Boons GJ, Bosch BJ, Huizinga EG, de Groot RJ, Human coronaviruses OC43 and HKU1 bind to 9-O-acetylated sialic acids via a conserved receptor-binding site in spike protein domain A. Proc. Natl. Acad. Sci. U.S.A 116, 2681–2690 (2019). [PubMed: 30679277]
43. Jiang F, Yang J, Zhang Y, Dong M, Wang S, Zhang Q, Liu FF, Zhang K, Zhang C, Angiotensin-converting enzyme 2 and angiotensin 1-7: Novel therapeutic targets. Nat. Rev. Cardiol 11, 413–426 (2014). [PubMed: 24776703]
44. Cantuti-Castelvetri L, Ojha R, Pedro LD, Djannatian M, Franz J, Kuivanen S, van der Meer F, Kallio K, Kaya T, Anastasina M, Smura T, Levanov L, Szirovicza L, Tobi A, Kailio-Kokko H, Osterlund P, Joensuu M, Meunier FA, Butcher SJ, Winkler MS, Mollenhauer B, Helenius A, Gokce O, Teesalu T, Hepojoki J, Vapalahti O, Stadelmann C, Balistreri G, Simons M, Neuropilin-1 facilitates SARS-CoV-2 cell entry and infectivity. Science 370, 856–860 (2020). [PubMed: 33082293]
45. Wang K, Chen W, Zhang Z, Deng Y, Lian JQ, Du P, Wei D, Zhang Y, Sun XX, Gong L, Yang X, He L, Zhang L, Yang Z, Geng JJ, Chen R, Zhang H, Wang B, Zhu YM, Nan G, Jiang JL, Li L, Wu J, Lin P, Huang W, Xie L, Zheng ZH, Zhang K, Miao JL, Cui HY, Huang M, Zhang J, Fu L, Yang XM, Zhao Z, Sun S, Gu H, Wang Z, Wang CF, Lu Y, Liu YY, Wang QY, Bian H, Zhu P, Chen ZN,

CD147-spike protein is a novel route for SARS-CoV-2 infection to host cells. Signal Transduct. Target. Ther 5, 283 (2020). [PubMed: 33277466]

46. Baggen J, Jacquemyn M, Persoons L, Vanstreels E, Pye VE, Wrobel AG, Calvaresi V, Martin SR, Roustan C, Cronin NB, Reading E, Thibaut HJ, Vercruysse T, Maes P, De Smet F, Yee A, Nivitchanyong T, Roell M, Franco-Hernandez N, Rhinn H, Mamchak AA, Ah Young-Chapon M, Brown E, Cherepanov P, Daelemans D, TMEM106B is a receptor mediating ACE2-independent SARS-CoV-2 cell entry. Cell 186, 3427–3442.e22 (2023). [PubMed: 37421949]
47. Devaraj SG, Wang N, Chen Z, Chen Z, Tseng M, Barretto N, Lin R, Peters CJ, Tseng C-TK, Baker SC, Li K, Regulation of IRF-3-dependent innate immunity by the papain-like protease domain of the severe acute respiratory syndrome coronavirus. J. Biol. Chem 282, 32208–32221 (2007). [PubMed: 17761676]
48. Chen X, Chou CY, Chang GG, Thiopurine analogue inhibitors of severe acute respiratory syndrome-coronavirus papain-like protease, a deubiquitinating and deISGylating enzyme. Antivir. Chem. Chemother 19, 151–156 (2009). [PubMed: 19374142]
49. Chuang SJ, Cheng SC, Tang HC, Sun CY, Chou CY, 6-Thioguanine is a noncompetitive and slow binding inhibitor of human deubiquitinating protease USP2. Sci. Rep 8, 3102 (2018). [PubMed: 29449607]
50. Dove B, Brooks G, Bicknell K, Wurm T, Hiscox JA, Cell cycle perturbations induced by infection with the coronavirus infectious bronchitis virus and their effect on virus replication. J. Virol 80, 4147–4156 (2006). [PubMed: 16571830]
51. He Y, Xu K, Keiner B, Zhou J, Czudai V, Li T, Chen Z, Liu J, Klenk HD, Shu YL, Sun B, Influenza A virus replication induces cell cycle arrest in G0/G1 phase. J. Virol 84, 12832–12840 (2010). [PubMed: 20861262]
52. Sui L, Li L, Zhao Y, Zhao Y, Hao P, Guo X, Wang W, Wang G, Li C, Liu Q, Host cell cycle checkpoint as antiviral target for SARS-CoV-2 revealed by integrative transcriptome and proteome analyses. Signal Transduct. Target. Ther 8, 21 (2023). [PubMed: 36596760]
53. Gupta RK, Mlcochova P, Cyclin D3 restricts SARS-CoV-2 envelope incorporation into virions and interferes with viral spread. EMBO J. 41, e111653 (2022). [PubMed: 36161661]
54. Tsang CM, Yip YL, Lo KW, Deng W, To KF, Hau PM, Lau VM, Takada K, Lui VW, Lung ML, Chen H, Zeng M, Middeldorp JM, Cheung AL-M, Tsao SW, Cyclin D1 overexpression supports stable EBV infection in nasopharyngeal epithelial cells. Proc. Natl Acad. Sci. U.S.A 109, E3473–E3482 (2012). [PubMed: 23161911]
55. Gheblawi M, Wang K, Viveiros A, Nguyen Q, Zhong JC, Turner AJ, Raizada MK, Grant MB, Oudit GY, Angiotensin-converting enzyme 2: SARS-CoV-2 receptor and regulator of the renin-angiotensin system: Celebrating the 20th anniversary of the discovery of ACE2. Circ. Res 126, 1456–1474 (2020). [PubMed: 32264791]
56. Gurley SB, Allred A, Le TH, Griffiths R, Mao L, Philip N, Haystead TA, Donoghue M, Breitbart RE, Acton SL, Rockman HA, Coffman TM, Altered blood pressure responses and normal cardiac phenotype in ACE2-null mice. J. Clin. Invest 116, 2218–2225 (2006). [PubMed: 16878172]
57. Zhao Y, Wang X, Wang Q, Deng Y, Li K, Zhang M, Zhang Q, Zhou J, Wang HY, Bai P, Ren Y, Zhang N, Li W, Cheng Y, Xiao W, Du HN, Cheng X, Yin L, Fu X, Lin D, Zhou Q, Zhong B, USP2a supports metastasis by tuning TGF-β signaling. Cell Rep. 22, 2442–2454 (2018). [PubMed: 29490279]
58. An R, Wang P, Guo H, Liuyu T, Zhong B, Zhang ZD, USP2 promotes experimental colitis and bacterial infections by inhibiting the proliferation of myeloid cells and remodeling the extracellular matrix network. Cell Insight 1, 100047 (2022). [PubMed: 37192862]
59. Dang F, Nie L, Zhou J, Shimizu K, Chu C, Wu Z, Fassl A, Ke S, Wang Y, Zhang J, Zhang T, Tu Z, Inuzuka H, Sicinski P, Bass AJ, Wei W, Inhibition of CK1ε potentiates the therapeutic efficacy of CDK4/6 inhibitor in breast cancer. Nat. Commun 12, 5386 (2021). [PubMed: 34508104]
60. Navarrete-Perea J, Yu Q, Gygi SP, Paulo JA, Streamlined tandem mass Tag (SL-TMT) protocol: An efficient strategy for quantitative (phospho)proteome profiling using tandem mass tag-synchronous precursor selection-MS3. J. Proteome Res 17, 2226–2236 (2018). [PubMed: 29734811]

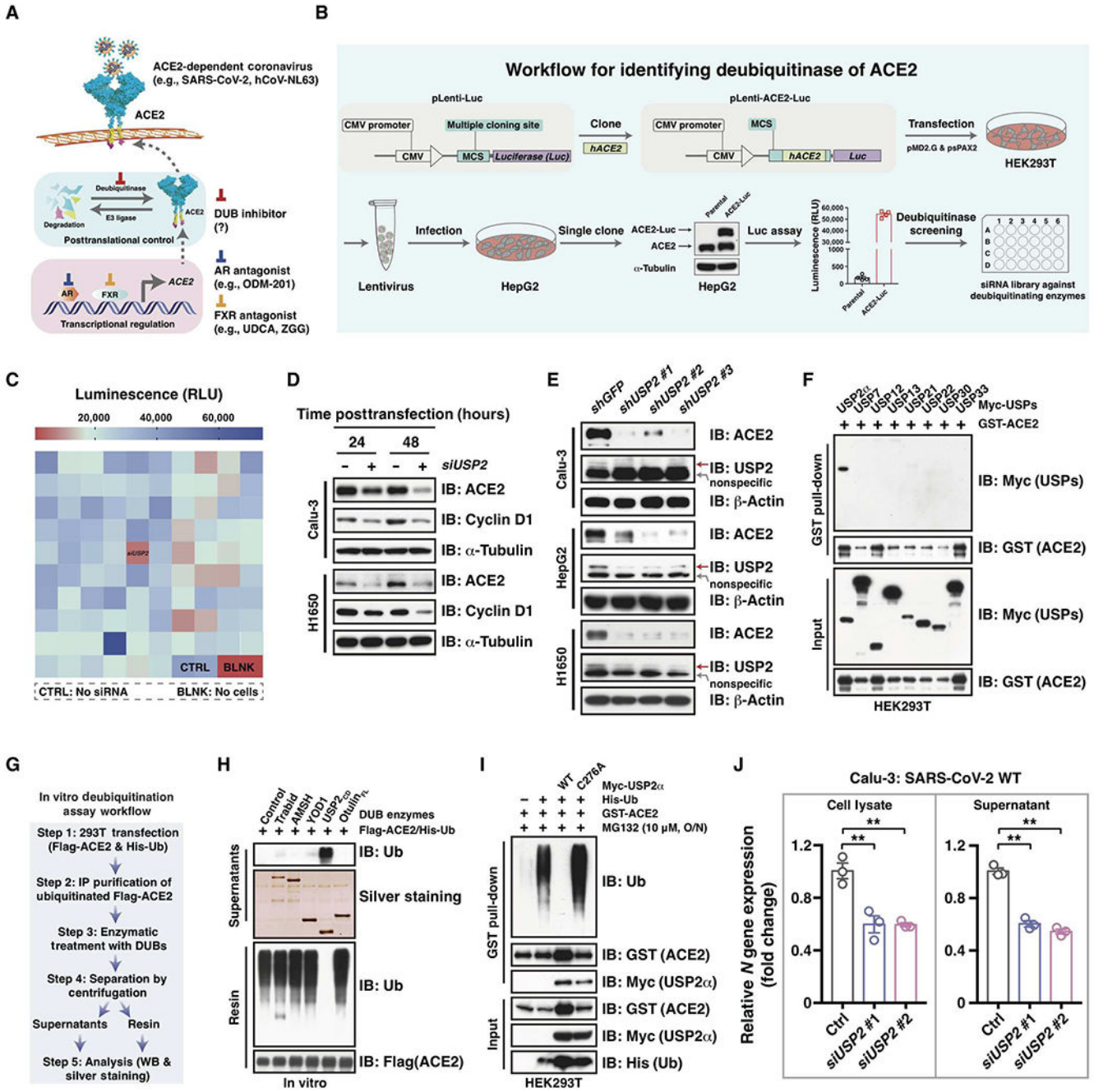

Fig. 1. USP2 is a physiological deubiquitinase of ACE2.

(**A**) A schematic model showing the regulation of *ACE2* expression at both transcriptional and posttranslational levels, along with strategies to combat viral infections through targeting *ACE2* expression. (**B**) Overview of the workflow for generating HepG2 cell line expressing a fusion gene of *ACE2* and *Luciferase* (*ACE2-Luc*) and the subsequent use of this cell line to identify the deubiquitinase of ACE2 through siRNA-based screening. (**C**) A heatmap showing the results of siRNA-based deubiquitinating enzyme screening. RLU, relative luminometer units. (**D**) Immunoblot analysis of ACE2 and cyclin D1 protein

abundance upon siRNA-mediated silencing of *USP2* in Calu-3 and H1650 cells. (**E**) Immunoblot analysis of ACE2 protein abundance upon shRNA-mediated silencing of *USP2* in the specified cell lines. The red arrows point to the USP2 band, whereas the lower bands are nonspecific. (**F**) Glutathione S-transferase (GST) pull-down assay examining the interaction between ACE2 and the indicated DUBs in HEK293T cells. (**G**) Workflow overview for in vitro deubiquitinating enzyme analysis, related to (H) and fig. S2F. IP, immunoprecipitation. WB, Western blot. (**H**) In vitro deubiquitination assay showing the impact of the indicated deubiquitinases on ACE2 ubiquitination. $USP2_{CD}$ represents the catalytic domain of USP2α. (**I**) Deubiquitination assay examining the role of both WT and catalytically inactive mutant (C276A) forms of USP2α in regulation of ACE2 deubiquitination. O/N, overnight. (**J**) Pseudovirus-based inhibition assay to assess the impact of *USP2* silencing on SARS-CoV-2 infection. The *P* values were calculated using Student's *t* test (two-sided), $n = 3$, $^{**}P < 0.01$.

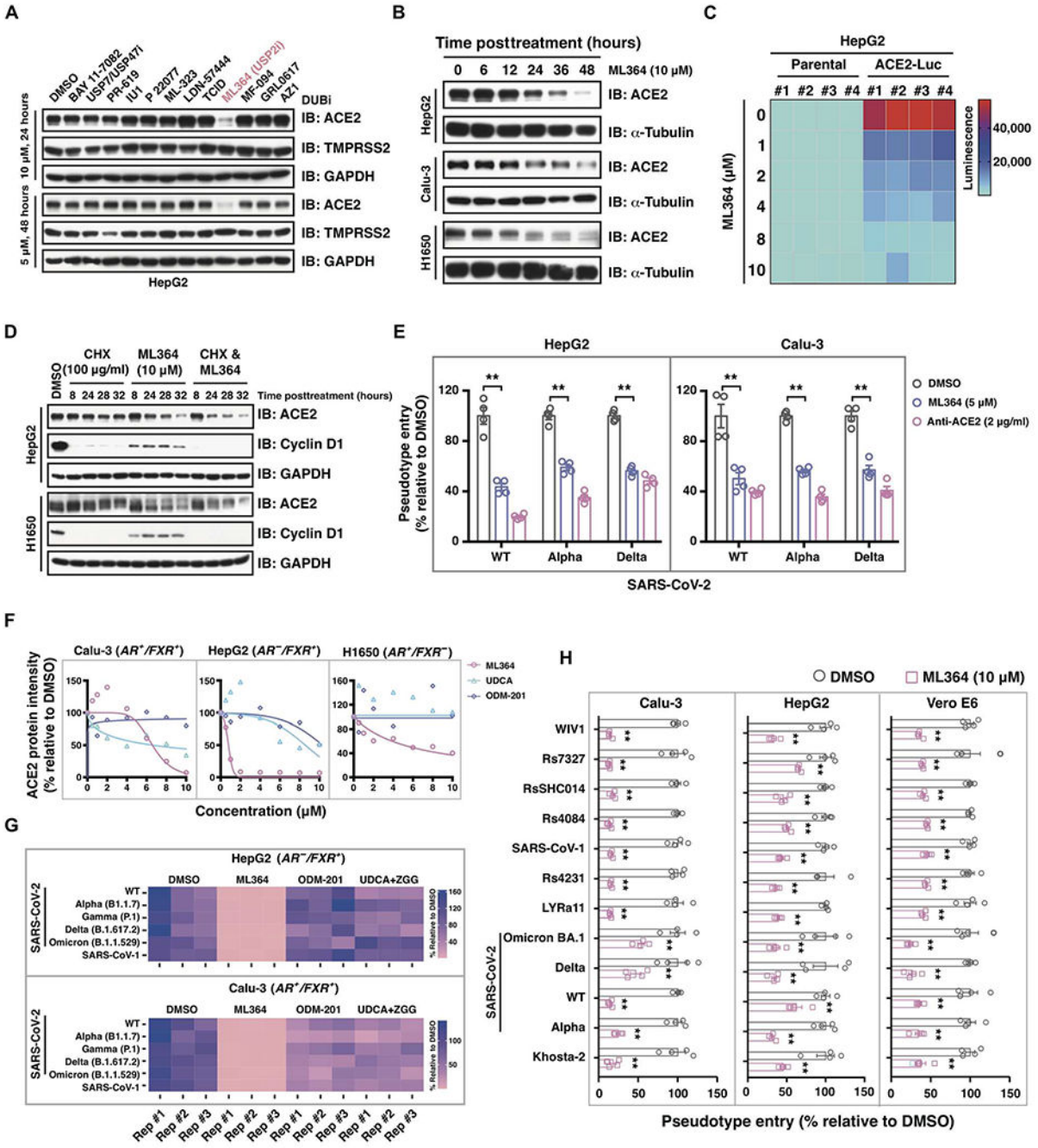

Fig. 2. USP2 inhibition with ML364 prevents ACE2-dependent pseudotype entry.

(**A**) Immunoblot analysis of ACE2 and TMPRSS2 protein abundance after treatment with the indicated deubiquitinase inhibitors in HepG2 cells. (**B**) Immunoblot analysis of ACE2 protein abundance after ML364 treatment across the specified cell lines. (**C**) Luciferase assay showing the ACE2-Luc signals after ML364 treatment. HepG2-ACE2-Luc cells were treated with ML364 at the indicated concentrations for 48 hours. (**D**) Immunoblot analysis of ACE2 and cyclin D1 protein abundance after the indicated treatment. GAPDH, glyceraldehyde phosphate dehydrogenase. (**E**) Pseudotype entry assay showing the impact

of ML364 on SARS-CoV-2 infection. HepG2 cells were preincubated with ML364 (5 μM) or anti-ACE2 antibody (AF933, 2 μg/ml) for 2 hours after being inoculated with pseudotyped SARS-CoV-2 WT, Alpha, or Delta strains for 48 hours. DMSO, dimethyl sulfoxide. (**F**) Quantification of the ACE2 protein intensity after ML364, UDCA, or ODM-201 treatment at the indicated concentrations for 48 hours, related to fig. S4F. (**G**) Pseudotype entry of the indicated viral strains after DMSO, ML364 (5 μM), UDCA (μM) plus ZGG (10 μM), or ODM-201 (10 μM) treatments in Calu-3 and HepG2 cells (n = 3). Cells were pretreated with the indicated compounds for 48 hours to induce ACE2 down-regulation, followed by inoculation with the corresponding pseudotypes for an additional 48 hours. (**H**) Pseudotype entry of the indicated viral strains in the context of DMSO or ML364 treatment (n = 4). Cells were pretreated with DMSO or ML364 (10 μM) for 1 hour before inoculation with the specified pseudotypes for an additional 48 hours. The P values were calculated using Student's t test (two-sided), $^{**}P < 0.01$.

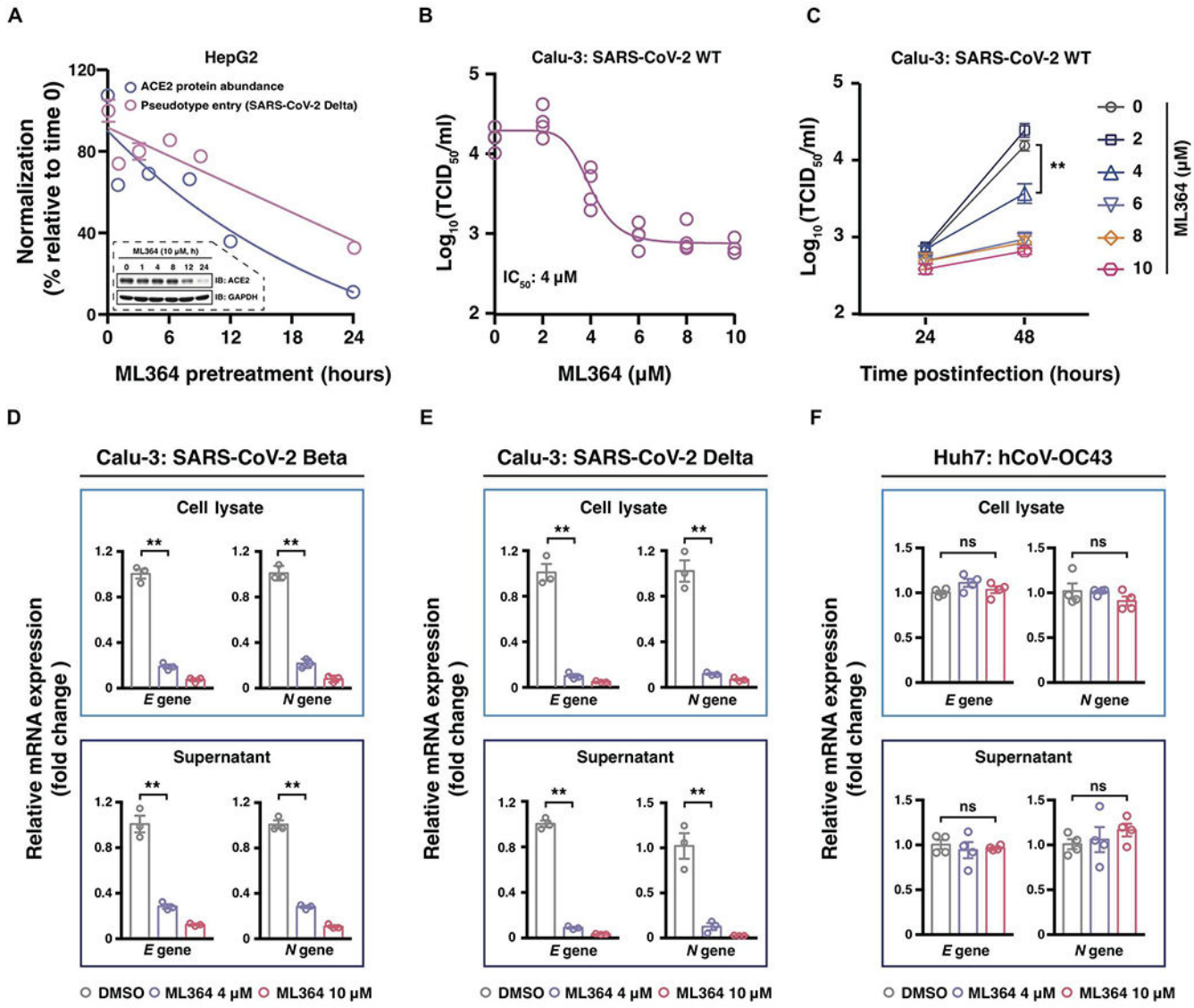

Fig. 3. ML364 is effective against SARS-CoV-2 WT and variants of concern in vitro.

(**A**) Effects of ML364 on ACE2 protein degradation and inhibition of pseudotyped SARS-CoV-2 entry. ACE2 protein intensity was quantified and normalized to the time point 0. For SARS-CoV-2 pseudotype entry assay, HepG2 cells were pretreated with 10 μM ML364 for the specified time intervals before SARS-CoV-2 Delta pseudotype inoculation, followed by an additional 24-hour incubation. (**B** and **C**) The 50% tissue culture infectious dose ($TCID_{50}$) assays to determine the IC_{50} of ML364 (B) and its impact on SARS-CoV-2 replication (C). Calu-3 cells were pretreated with ML364 at the indicated concentrations for 48 hours before exposure to the SARS-CoV-2 WT at a multiplicity of infection (MOI) of 0.01. Cell culture supernatants were harvested at 48 hours (B) or at the indicated time points (C) postinfection to determine viral titers using the $TCID_{50}$ assay. (**D** to **F**) Reverse-transcription quantitative polymerase chain reaction (RT-qPCR) analyses of *E* and *N* genes from SARS-CoV-2 Beta (D), Delta (E), and hCoV-OC43 viruses (F). For SARS-CoV-2 studies, Calu-3 cells were pretreated with ML364 at the indicated concentration for 48 hours

before exposure to authentic SARS-CoV-2 strains with an MOI of 0.1 for an additional 48 hours. For the hCoV-OC43 experiment, Huh7 cells were preinfected with HCoV-OC43 at a MOI of 2 for 24 hours, after being treated with DMSO, ML364 (4 μM), or ML364 (10 μM), respectively, for an additional 48 hours. The *P* values were calculated using Student's *t* test (two-sided), $^{**}P < 0.01$, $n = 3$ or 4 per group. Experiments related to authentic viral studies were performed once and repeated using three different authentic SARS-CoV-2 viral strains and four different treatment regimens as shown in figs. S6 and S7. ns, no significant difference.

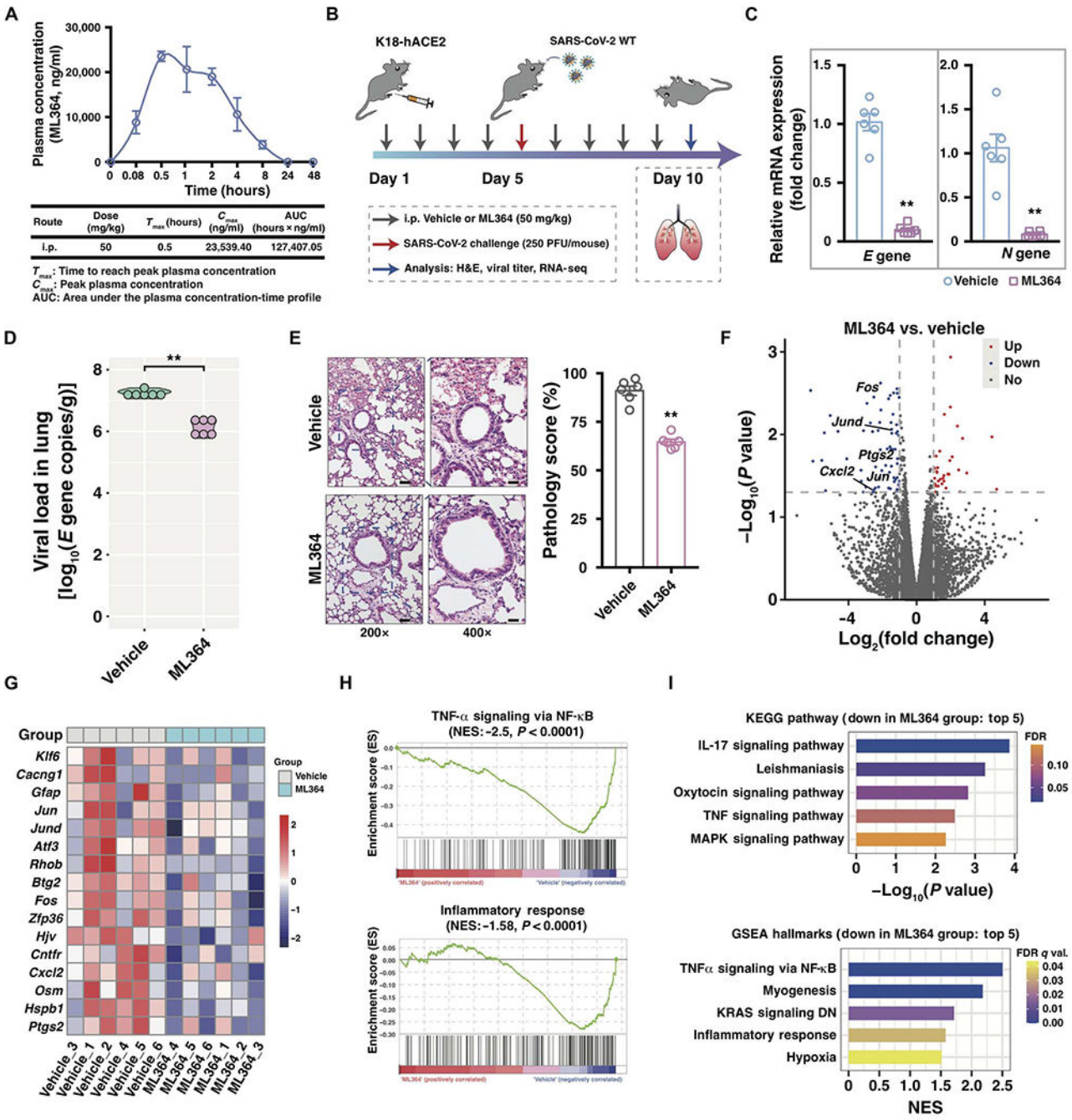

Fig. 4. ML364 exhibits protective efficacy against SARS-CoV-2 in vivo.

(**A**) Pharmacokinetic properties of ML364 in male C57BL/6 mice. i.p., intraperitoneal. (**B**) A graphical representation of the in vivo study design for evaluating the protective efficacy of ML364 against SARS-CoV-2 infection (n = 6). PFU, plaque-forming units. (**C**) The mRNA expression of SARS-CoV-2 *E* and *N* genes in the lungs derived from mice treated with vehicle and ML364. (**D**) The viral loads in the lungs of mice administered with the vehicle and ML364. (**E**) Representative images of H&E staining of the lung tissues treated with vehicle or ML364. Scale bars, 50 μm (200×) and 20 ϰm (400×). The bar graph on the

right showing the lung pathology score for each mouse. (**F** to **I**) The total mRNA from the lungs of mice harvested above was extracted, followed by a comprehensive gene expression analysis using RNA-seq. The differential gene expressions are visually represented in the volcano plot (F), whereas the heatmap depicts the expression patterns of genes associated with inflammation (G). The pathways of tumor necrosis factor–α (TNF-α) signaling and inflammatory response were analyzed through GSEA enrichment plots (H), and the top five down-regulated KEGG pathways and GSEA hallmarks in the ML364-treated group were analyzed using GSEA (I). NES, normalized enrichment score; FDR, false discovery rate. *P* values for the GSEA analyses were computed using Kolmogorov-Smirnov tests, whereas the *P* values for two-group comparisons were calculated using a two-sided Student's *t* test, $^{**}P < 0.01$. Experiments presented in this figure were conducted once with six replicates in each treatment. NFκB, nuclear factor κB; IL-17, interleukin-17; MAPK, mitogen-activated protein kinase; KRAS, kirsten rat sarcoma virus; DN, down-regulated.

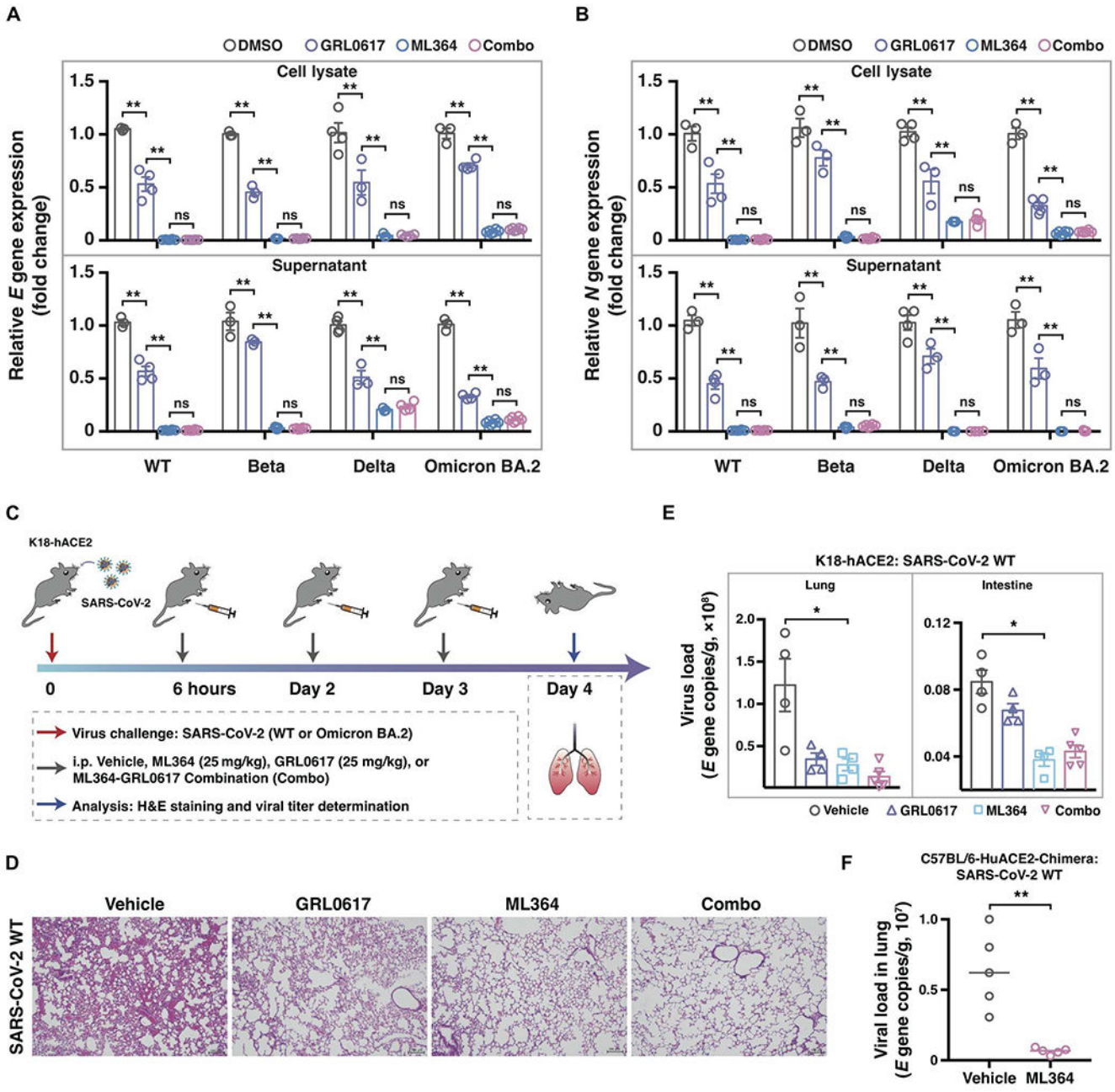

Fig. 5. Therapeutic treatment with ML364 reduces severity of SARS-CoV-2 infection.

(**A** and **B**) RT-qPCR analysis of *E* (A) and *N* (B) genes of SARS-CoV-2 WT, Beta, Delta, and Omicron BA.2 strains in the context of the specified treatments ($n = 3$ to 6). Calu-3 cells were preinfected with WT, Beta, Delta, or Omicron BA.2 strains of SARS-CoV-2 with an MOI of 0.1 for 1 hour before treatment with DMSO, GRL0617 (10 μM), ML364 (10 μM), or GRL0617-ML364 combination (Combo), respectively, for an additional 48 hours. (**C**) A schematic illustration for the design of the in vivo study to investigate the therapeutic potential of ML364 for treating SARS-CoV-2 WT (250 plaque-forming units per mouse) and Omicron BA.2 infection (400 plaque-forming units per mouse). (**D**) Representative

images of H&E staining of the lung tissues obtained from designated groups. Scale bars, 100 μm. (**E**) The viral loads of SARS-CoV-2 in the lung and intestinal tissues acquired from specified groups ($n = 4$ to 5). (**F**) The viral loads of SARS-CoV-2 in the lung tissues of HuACE2-Chimera mice treated with vehicle and ML364, respectively ($n = 5$). The P values were calculated using Student's t test (two-sided), $^{*}P < 0.05$ and $^{**}P < 0.01$. Experiments depicted in this figure were conducted as a single experiment.

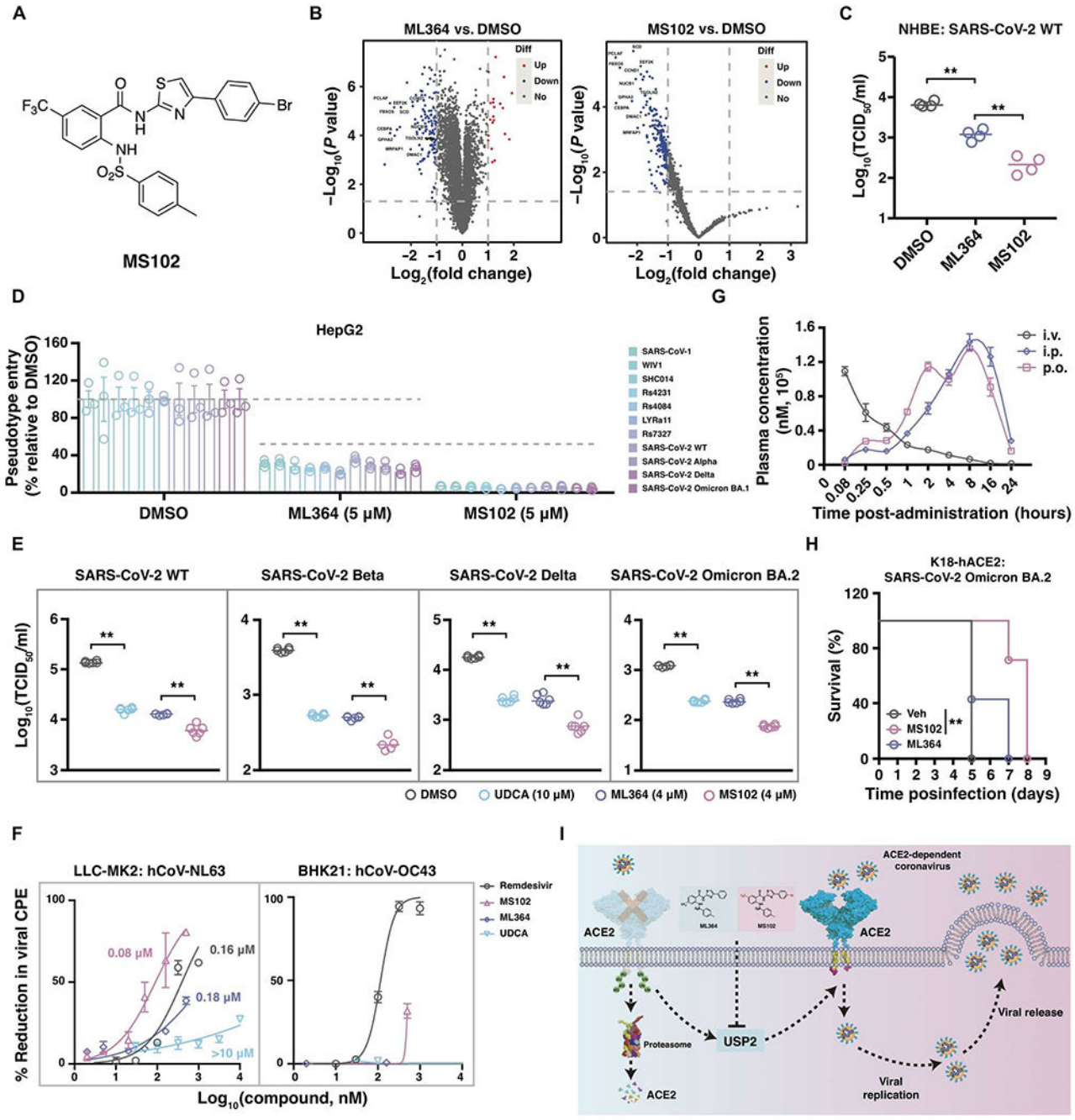

Fig. 6. MS102 is an oral USP2 inhibitor with enhanced antiviral activity.

(**A**) The chemical structure of MS102 is shown. (**B**) Volcano plots show the differential protein abundance changes in response to ML364 or MS102 treatment in HepG2 cells. HepG2 cells were treated with 10 μM ML364 or MS102 for 24 hours. Total proteins were extracted, and protein abundance was determined using TMT-based proteomic analysis. (**C**) $TCID_{50}$ assay showing the efficacy of ML364 and MS102 in preventing infection of NHBE cells by SARS-CoV-2 WT ($n = 4$). NHBE cells were preinfected with the SARS-CoV-2 WT with an MOI of 0.01 for 1 hour before exposure to DMSO, ML364

(10 μM), or MS102 (10 μM) for an additional 48 hours. (**D**) Pseudotype entry of specified viruses in the context of DMSO, ML364, or MS102 treatments ($n = 3$). HepG2 cells were pretreated with DMSO, ML364 (5 μM), or MS102 (5 μM) for 24 hours, followed by incubation with indicated pseudotypes for an additional 48 hours. (**E**) $TCID_{50}$ assay comparing the efficacy of UDCA, ML364, and MS102 in preventing Calu-3 cells from being infected by specified SARS-CoV-2 viral strains ($n = 6$). Calu-3 cells were preinfected with WT, Beta, Delta, or Omicron BA.2 strains of SARS-CoV-2 with an MOI of 0.1 for 1 hour before exposure to DMSO, UDCA (10 μM), ML364 (4 μM), or MS102 (4 μM) for an additional 48 hours. (**F**) Cytopathic effect (CPE) assay to assess the efficacy of the indicated compounds against authentic hCoV-NL63 and hCoV-OC43 viruses. (**G**) The pharmacokinetics of MS102 in male C57BL/6 mice after a single administration through three different routes: intraperitoneal (i.p., 50 mg/kg), intravenous (i.v., 5 mg/kg), and oral (p.o., 50 mg/kg). (**H**) A survival study to evaluate the protective efficacy of ML364 and MS102 in K18-hACE2 transgenic mouse model. The *P* value was calculated using the log-rank (Mantel-Cox) test. (**I**) A graphic model showing the molecular mechanism through which USP2 inhibition prevents viral infections by destabilizing host ACE2 protein. Protein structures are as follows: ACE2 (6 M18) and human 26S proteasome (5L4G). The *P* values were calculated using Student's *t* test (two-sided), $^{**}P < 0.01$.